Dear Editor,

We greatly appreciate all of editor and reviewers' comments and suggestions which have been accepted in revised version of our manuscript: Dynamics of environmental conditions during a decline of a Cymodocea nodosa meadow (bg-2019-484). We believe we have satisfactorily addressed them.

Associate Editor Decision: Reconsider after major revisions (29 Mar 2020) by Minhan Dai

Comments to the Author:

Re: g-2019-484 "Dynamics of environmental conditions during a decline of a Cymodocea nodosa meadow" by Mirjana Najdek et al.

Dear authors,

I went through both your MS and your interactive responses to the reviews. I encourage you to submit a thoroughly revised MS by carefully consider these reviews. In particular, I urge you to address the critical comments on light raised by both reviewers.

When you submit your revised MS, you need to provide a point-to-point letter explaining how you address the comments and concerns from the reviewers. Your revised MS will be sent out for further reviews.

Sincerely,

Minhan Dai

Editor

Please, find below the short list of changes we made in our revised manuscript and a point-to-point letter explaining how we addressed the comments and concerns from the reviewers:

- *In Abstract the sentence concerning light availability decrease in April 2018 was rewritten. The sentence about recovery of the below-ground tissue was rephrased.*
- *In Introduction the newer literature about preservation of marine diversity and carbon sequestration was provided.*
  Introduction about seagrass meadows in Adriatic and research gap was added.
- *In Materials and Methods a map was provided (now Fig S1). The sampling dates and depths of C. nodosa were included.*
- *The Discussion has been re-arranged.*
- *The Conclusion has been rewritten as advised.*
- *Figure 4…The years are annotated and an explanation is added in the legend*
- *Supplementary material…A sampling map was inserted as Fig S1.*

Please find our point-by-point response to each reviewer's comments below:

Interactive comment on "Dynamics of environmental conditions during a decline of a Cymodocea nodosa meadow" by Mirjana Najdek et al.

Anonymous Referee #1

The authors investigated the dynamics of environmental conditions during a decline of a Cymodocea nodosa meadow in the northern Adriatic Sea, analyzed the correlation between those physicochemical and biological parameters, and concluded that the reduced light availability and following photosynthesis was the most likely reason leading to the decay of seagrass meadow. The experiments seem to be conducted carefully and the results were thoroughly discussed. This study supplies helpful information on understanding the decline of seagrass globally. However, there are some points that the authors need to attend to before it can be published in Biogeosciences.

I have two general concerns about this study.

COMMENT: The loss of seagrass meadow is attributed to reduced light availability and thus photosynthesis in this study. However, it seems that there is no direct data to support this conclusion. Have the light intensity in water column and photosynthetic rate of seagrasses were measured? The solar radiation in April should not be the lowest level compared to other months.

RESPONSE: *Light intensity in the water column and photosynthetic rates of seagrass were not measured and there are no direct data to support this conclusion. However, indirectly from the data, the reduction of available light to the C. nodosa meadow in April 2018 was indicated by a visible increase in turbidity of the water column, due to an increased concentration of particulate matter of terrigenous origin and sediment resuspension. Terrigenous input in combination with sediment resuspension covered the meadow with sediment; thereby significantly reducing the amount of light accessible to the plant. Indeed, the solar radiation in April should not be at the lowest level compared to other months, therefore we would rule out the decrease in solar radiation as a potential trigger of the seagrass decay in April 2018.*

COMMENT: The authors mentioned that from July 2017 to March 2018, C. nodosa successfully adapted to the changes of environmental conditions and prevented H2S accumulation by its re-oxidation, supplying the sediment with O2 from the water column and/or leaf photosynthesis. Then why did not C. nodosa adapt to the environmental changes from April 2018 onwards? I am wondering that the decline of seagrass meadow in the northern Adriatic Sea is a natural process or caused by other drivers?

RESPONSE: *We believe that already in April 2018, C. nodosa received the amount of light below the minimum required for photosynthesis, as suggested by an increase in LA/ALA ratio > 1 (as conversion of LA to ALA declines in dark being completely inhibited by anaerobiosis). Besides reduced photosynthesis and therefore supply of the below-ground tissue with oxygen, a depletion of oxygen due to intense oxidation of H_2S occurred in the sediment, thus creating anoxic conditions in most of the rooted areas. Most likely, this change in April 2018 drastically and irreversibly compromised the survival of the meadow. From April 2018 onwards, C. nodosa didn't reestablish photosynthesis and continued to lose shoots and overall biomass, while at the same time in the sediment, the concentration of H_2S increased considerably, which, due to lack of oxygen, penetrated the plant and caused the meadow die-off. We would exclude that the process in Saline Bay was natural, because several geographically nearby meadows didn't display a similar pattern of regression.*

COMMENT: Line 22 Why did light availability decrease in April 2018?

RESPONSE: *The available light to the C. nodosa was reduced due to increased seawater turbidity resulted from combined effect of terrigenous input, sediment resuspension and elevated autotrophic biomass. The sentence was rewritten and amended.*

CHANGE (Page 2, Lines 23 – 26): *The C. nodosa decline was most likely triggered in April 2018 when light availability to the plant was drastically reduced. Such conditions resulted from increased seawater turbidity due to terrigenous input, sediment resuspension and elevated autotrophic biomass.*

COMMENT: Line 30 The data in Figure 2 did not show the recovery of the below-ground tissue?

RESPONSE: *We agree with this comment. The sentence in the Abstract was rephrased.*

CHANGE (Page 2, Lines 33 – 34): *The influx of oxygenated waters in September 2018 led to the re-establishment of H_2S oxidation in the sediment and the remaining of the below-ground tissue.*

COMMENT Line 37 Better to supply latest literature as there are loads?

RESPONSE: *The following literature has been added*

CHANGE (Page 3, Lines 42 – 43): *Duarte, C.M., Kennedy, H., Marbà, N., Gacia, E., Fourqurean, J.W., Beggins, J., Barrón, C., Apostolaki, E.T.: Seagrass community metabolism: Assessing the capacity of seagrass meadows for carbon burial: Current limitations and future strategies. Ocean Coast. Manag., 83, 32-38, 2013. Samper-Villarreal, J., Lovelock, C.E., Saunders, M.I., Roelfsema, C., and Mumby, P.J.: Organic carbon in seagrass sediment is influenced by seagrass canopy complexity, turbidity, wave height, and water depth. Limnol. Oceanogr., 61, 938-952, 2016.*

COMMENT: Line 41 Add a comma after matter… *a comma was added*.

COMMENT: Line 85 A introduction about seagrass meadows in Saline Bay or Adriatic Sea should be supplied here. Meanwhile, it would be helpful to add research gap here.

RESPONSE: *Introduction about seagrass meadows in Adriatic and research gap was added.*

CHANGE (Page 4, Lines 90 – 100): *The seagrass Cymodocea nodosa (Ucria) Ascherson is widely distributed and common species throughout the Mediterranean (Terrados and Ros 1992; Pedersen et al., 1997; Cancemi et al., 2002; Agostini et al., 2003). For the northern Adriatic, however, only sparse data are available on the standing crop, seasonal dynamics or natural/anthropogenic pressures supporting the ecological or conservation status of C. nodosa meadows (Zavodnik et al., 1998; Orlando-Bonaca et al., 2015). Although C. nodosa show large phenotypic plasticity adapting to diverse natural and anthropogenic stressors by physiological and morphological adaptations, a severe decline has been reported during the last decades in coastal areas (Orth et al., 2006; Short et al., 2011; Tuya et al., 2002; 2014), including the northern Adriatic (Orlando-Bonaca et al., 2015; 2019). One of these declines is documented in our study performed in Saline Bay (northern Adriatic Sea) from July 2017 to October 2018.*

New references: Orlando-Bonaca, M., Francé, J., Mavrič, B., Grego, M., Lipej, L., Flander Putrle, V., Šiško, M., and Falace, A.: A new index (MediSkew) for the assessment of the Cymodocea nodosa (Ucria) Ascherson meadow's status. Mar. Environ. Res., 110, 132-141, 2015.

Orlando-Bonaca, M., Francé, J., Mavrič, B., and Lipej, L.: Impact of the Port of Koper on Cymodocea nodosa meadow. Annales, 29, 187-194, 2019.

Short, F.T., Polidoro, B., Livingstone, S.R., Carpenter, K.E., Bandeira, S., Bujang, J.S., Calumpong, H.P., Carruthers, T.J.B., Coles, R.G., Dennison, W.C., Erftemeijer, P.L.A., Fortes, M.D., Freeman, A.S., Jagtap, T.G., Kamal, A.M., Kendrick, G.A., Kenworthy, W.J., La Nafie, Y.A., Nasution, I.M., Orth, R.J., Prathep, A., Sanciangco, J.C., van Tussenbroek, B., and Vergara, S.G.: Extinction risk assessment of the world's seagrass species. Biol. Conserv., 144, 1961-1971, 2011.

Tuya, F., Martín, J.A., and Luque, A.: Impact of a marina construction on seagrass bed at Lanzarote (Canary Islands). J. Coast. Conserv., 8, 157-162, 2002.

Tuya, F., Ribeiro-Leite, L., Arto-Cuesta, N., Coca, J., Haroun, R., and Espino, F.: Decadal changes in the structure of Cymodocea nodosa seagrass meadows: Natural vs. human influences. Estuar. Coast. Shelf Sci., 137, 41-49 (2014).

COMMENT: Line 98 Better to supply a map for the study site.

RESPONSE: *A map is now added as Fig S1* **(Page 5, Line 110)** *and provided in Supplementary material* **(Page 5)**

COMMENT: Line 116 Sampling time/frequency needs to be stated. What is the depth for C. nodosa living?.

RESPONSE: *The sampling dates and depths of C. nodosa were included*

CHANGE (Page 5, Line 126 and 128): *The sampling was performed for 15 months from July 2017 to October 2018. C. nodosa (3 - 4 m of depth) was collected together with rhizomes, roots and macroalgae by divers using the quadrat sampling method.....*

COMMENT: Line 320 This is true as shown in the green macroalgae Ulva linza (Gao et al. 2018 Food Chemistry, 2018, 258: 71-78).?

RESPONSE: *The reference was added in the text* **(Page 12, Line 331)** *and listed in References.*

COMMENT: Line 386 What are these prokaryotic organism?

RESPONSE: *Prokaryotic organisms are Bacteria and Archaea from 0.2 – 2 µm, stained with DAPI and counted by epifluorescence microscopy.*

COMMENT: Lines 485-487 How did you know it? Any data or literature to support this speculation??

RESPONSE: *In July and August 2017 the leaves were short with visible signs of bites, so we assumed that significantly lower biomass in these two months was the result of grazing*

activity of herbivores. Generally, the meadows have been shown to be an important source of food for herbivores. We rephrased the sentences to avoid misleading interpretation and have added the references that support biomass loss by herbivory in C. nodosa.

CHANGE (Page 17, Lines 501 – 504)*: In Saline Bay, the maximum biomass was measured in October 2017. This shift from summer to early autumn was most likely due to an intense grazing activities (Cebrian et al., 1996; Valentine and Duffy, 2006) suggested by a prevalence of visibly grazed leaves during July and August.*

New references: Cebrian, J., Duarte, C.M., and Marbà, N.: Herbivory on the seagrass Cymodocea nodosa (Ucria) Ascherson in contrasting Spanish Mediterranean habitats. J. Exp. Mar. Biol. Ecol., 204, 103-111, 1996

Valentine, J.F., and Duffy, J.E.: The central role of grazing in seagrass ecology. In: Seagrasses: Biology, Ecology and Conservation, Springer, Netherlands, pp 431-501, 2006.

COMMENT: Line 680 Conclusion should not be a repetition of Abstract. The purpose of a conclusion is to tie together, or integrate the various issues, findings, arguments etc., covered in the body of the paper, and to make comments upon the meaning of all of it. This includes noting any implications resulting from your discussion of the topic, as well as recommendations, forecasting future trends, and the need for further research.

RESPONSE*: The Conclusion has been rewritten.*

CHANGE (Page 24, Lines 717 – 729)*: Our results provide insights into the interaction of multiple stressors that have led to the meadow decay, triggered in the sensitive recruitment phase of meadow growth. Even after the improvement of the sediment conditions by the end of the summer 2018, C. nodosa was not able to recolonize its previously occupied areas. This finding combined with a visible alteration of the water column and sediment indicates a considerable loss of the C. nodosa habitat. Further research is needed to examine the fate of Saline Bay meadows and an eventual recolonization of the area. Beyond seagrass itself, this loss had extensive consequences as it has endangered many species that depend on seagrass for food, shelter and nursery. Given the lack of data on the ecological and conservation status of the still numerous seagrass meadows along the northern Adriatic coast, the identification and monitoring of the main pressures acting on them are needed to protect such valuable habitats from degradation and extinction.*

COMMENT Line 950 Please annotate which year for the months and explain why it ends in Feb in the legends.

RESPONSE*: The years are annotated and an explanation is added in the Figure 4 legend.*

CHANGE (Page 39, Line 1012)*: Figure 4. The contribution of macroalgal phyla in a meadow and total macroalgal biomass; after February 2018 macroalgae were no longer present in the C. nodosa meadow.*

Interactive comment on "Dynamics of environmental conditions during a decline of a Cymodocea nodosa meadow" by Mirjana Najdek et al.

The paper entitled "dynamics of environmental conditions during a decline of cymodocean nodosa meadow" reported biomass changes of the seagrass along with environmental changes in both seawater and sediments during one year period of 2017 to 2018. The results showed that C. nodosa successfully adapted to the changes of environmental conditions and prevented H2S accumulation by its re-oxidation, supplying the sediment with O2 from the water column and/or leaf photosynthesis, implying that the C. nodosa die-off would be most likely caused in April 2018 by a reduction of light availability. Unfortunately, solar irradiances changes either at the surface of water column or in water were not supplied. Especially, the light levels during investigation periods were not provided. Attenuation of light in water during different seasons with different amounts of PM can be directly link to photosynthetic performance of the seagrass. While the authors showed that in the sediment, depletion of oxygen due to intense oxidation of H2S led to anoxic conditions in most of the rooted areas. This could negatively affect respiration of the plant root, therefore, its growth. With reduced growth capacity, high concentrations of H2S were observed in the sediment cores and bottom waters. This is an interesting result indicating the relationship of H2S levels with photosynthetic O2 evolution. Generally speaking, the paper has scientific significance, and is suitable to be accepted to BG after revision.

Specific comments:

COMMENT: Daily sunlight doses should be in parallel with water temperature, and should be provided, which can be easily obtained from local meteorological stations if the authors did not measure.

RESPONSE: *We are aware that the temperature of natural water bodies varies in response to diurnal and seasonal changes in solar radiation. Our temperature data showed no unusual diurnal and/or seasonal pattern. Therefore, it could be reasonably assumed that during the study period there was no big difference in the amount of solar radiation received by the sea. Also we believe that solar radiation data from a meteorological station would not help here. From reporting solar radiation measured in the lower atmosphere (as typically done by meteo-stations), the solar radiation reaching the seagrass meadow in this coastal system cannot be extrapolated. Underwater solar radiation measurements would be required which, unfortunately, we don't have. The penetration of light in the water column, which regulates photosynthesis, is strongly influenced by the transparency of the water. The attenuation of light in the water column and therefore, the reduced availability of light required for C. nodosa photosynthesis in April 2018 was attributed to the measured increased concentration of particulate matter in the water column due to the resuspension of sediment and influx from the land, as well as simultaneous sediment redeposition on the leaves. A sentence linking the reduction of available light to the meadow with increased water turbidity in April 2018 has been added to Abstract.*

CHANGE (Page 2, Lines 23 – 26): *The C. nodosa decline was most likely triggered in April 2018 when light availability to the plant was drastically reduced due to increased seawater turbidity that resulted from increased terrigenous input combined with resuspension of sediment and elevated autotrophic biomass.*

COMMENT: Decline of the seagrass meadow can hardly be attributed to light availability, grazing pressure or others. It must be a result of multiple drivers impact. Therefore, the discussion should be re-sorted and holistically analyzed.

RESPONSE: We agree that the decline of the seagrass meadow in Saline Bay was the result of multiple drivers' impact. It all began with the increased water turbidity which weakened the plant and made it susceptible to other stressors such as lack of oxygen and H2S penetration within the plant tissue. Marks of visible grazing were only observed in July and August 2017 and not in April 2018 when the die-off was triggered. For this reason we did not include grazing as one of the main drivers in the decline of C. nodosa meadow. The Discussion has been re-arranged according to the periods of regular growth of the C. nodosa meadow (July 2017 – March 2018) and its decay (April-August 2018). We believe that in this way we presented more clearly the meadow decline as a result of multiple drivers' cascading impact. Also, in this way the repeated wordings in the sentences and paragraphs were avoided, as recommended, and this resulted in shorter discussion.

CHANGE (Pages 16 – 23, Lines 479 – 698): Saline bay is a shallow, highly dynamic coastal area characterized by frequent turbid waters due to the combined effect of land run-off and wind-driven resuspension of the fine sediment. Nutrients and Chl a (as a proxy for autotrophic biomass) varied in the ranges characteristic for the oligotrophic coastal waters off Rovinj (Ivančić et al., 2018). The dynamics of particulate matter was associated with freshwater input. The higher contribution from autochthonous sources was observed during the increases of autotrophic biomass. However, only in September 2017, this increase was supported by nutrients from the water column, while the other increases were likely connected to bottom waters where phytoplankton could have been supplied with nutrients through sediment resuspension. The considerable increase in the particulate matter of terrigenous origin from April to August 2018 suggested the enhanced land run-off in that period.

In temperate Mediterranean coastal waters C. nodosa meadows show a clear unimodal annual growth cycle, reaching maximum development in summer, minima during winter and a particularly active phase in spring (Terrados and Ross, 1992; Zavodnik et al., 1998; Agostini et al., 2003). In Saline Bay, the maximum biomass was measured in October 2017. This shift from summer to early autumn was most likely due to an intense grazing activities (Cebrian et al., 1996; Valentine and Duffy, 2006) suggested by a prevalence of visibly grazed leaves during July and August 2017. A minimum growth occurred during late autumn/winter, as commonly observed. However, during the spring of 2018, phenological parameters continued to decrease despite established favorable environmental conditions for growth, i.e. increase in water temperature, intensity and period of solar radiation. This decrease continued until the complete extinction of the aboveground tissue in August 2018. The below-ground tissue followed a similar trend, but with less expressed changes. Still, their recognizable remnants were found after the loss of above-ground tissues.

Organic matter and closely correlated total lipids in the sediment of C. nodosa rooted area changed significantly throughout the investigated period, in contrast to organic matter in non-vegetated sediment. Nevertheless, considerable similarity in the quality and degradation of lipid matter at both, the vegetated and the non-vegetated sites indicates an important contribution of detritus imported from the meadow as a source of organic matter for prokaryotes in non-vegetated sediments. This close coupling could be expected due to sites proximity and lower organic content of the non-vegetated sediment, which should enhance the dependence of prokaryotes on the imports of seagrass detritus from the adjacent meadows (Holmer et al., 2004). Significant enrichment of C. nodosa sediment with unsaturated, more labile components only during abundant growth of meadow could be explained by more efficient entrapment of seston material within the meadow (Gacia and Duarte, 2001). Such easily utilizable organic matter, including dissolved monomeric carbohydrates, leaching out during decomposition of C. nodosa leaves stimulated prokaryotic growth as previously observed (Peduzzi and Herndl, 1991).

From July 2017 to March 2018, an adaptation of C. nodosa leaves to the decreasing light and temperature occurred. Until October 2017, the temperature of the water column was still optimal for elongation of the leaves and biomass increase, while the ambient light intensities were continuously decreasing. An additional reduction of available light might occur from the self-shading effect due to high canopy biomass, and/or shading due to epiphytic macroalgae growth. Desaturation of low and fairly invariable lipids during the most active growth phase suggested an increase in the membrane fluidity to optimize photosynthetic activity under low light conditions. Such physiological adaptation was found in seagrasses living along a depth gradient (Beca-Carretero et al., 2019) and macroalgae in contrasting seasons (Schmid et al., 2014). In late autumn 2017, the decrease in desaturation indicated a reduced fluidity and activity of photosynthetically active membranes (Quigg et al., 2006; Wacker et al., 2016). This was associated with a decreased abundance of shoots and aboveground biomass. By shedding leaves and shoots the plant further balances metabolic requirements and mobilize energy from the carbohydrate reserves stored in the below-ground tissue (Alcoverro et al., 2001; Lee et al., 2007). During the winter, due to a sharp and continuous decrease in water temperature, rapid desaturation of increasing lipids provided a cold resistance, as regularly observed in algae and plants (Terrados and Lopezjimenez, 1996; Iveša et al., 2004; Upchurch, 2008).

In a healthy seagrass meadow, the oxygen generated by photosynthesis is transported to below-ground tissues to maintain an oxic microsphere around roots and rhizomes, re-oxidize sulfide to non-toxic S^0, thus preventing an invasion of H_2S into the plant and root anoxia (Pedersen et al., 1998; Holmer et al, 2005). S^0 was found in the C. nodosa below-ground tissue during the entire investigation period, as regularly observed in seagrasses living in

sulfidic sediments (Holmer and Hasler-Sheetal, 2014; Hasler-Sheetal and Holmer, 2015). The relatively low accumulation of H_2S (< 30 µM) during the summer and early autumn 2017 indicated that H_2S was apparently rapidly recycled within the rooted area via re-oxidation by O_2 to S^0 and/or removal by precipitation with iron compounds. Most of S^0 was found in oxic layers or suboxic/anoxic boundaries, being in ranges typical for sulfidic coastal sediments (Troelsen and Jørgensen, 1982; Panutrakul et al., 2001; Pjevac et al., 2014). The oxidation of H_2S could occur spontaneously by chemical reaction with free oxygen or mediated by sulfide-oxidizing bacteria surrounding or being attached to seagrass roots (Jørgensen, 1977; Cucio et al., 2016; Ugarelli et al., 2017; Fahimipour et al., 2017). In November, due to the degradation of organic matter, reduced oxygen production and leakage in the rooted zone caused by C. nodosa senescence, the re-oxidation capacity of the sediment was greatly decreased. This resulted in considerable accumulation of H_2S (> 100 µM) which extended up to the sediment surface. In winter and early spring, H_2S production generally decreased, likely due to the reduced activity of sulfate reducing prokaryotes at lower temperatures, and the sediment gradually shifted towards a more oxidized state. H_2S detected even in within the oxic sediment and in the rooted area could be attributed to the sediment heterogeneity and the presence of reducing micro-niches where anaerobic metabolism could occur regardless of surrounding redox conditions (Jørgensen, 1977; Frederiksen and Glud, 2006).

In April 2018, C. nodosa had been most probably exposed to increased siltation, due to an increase in terrigenous input combined with resuspension of sediment provoking elevated autotrophic growth. The intensive siltation is associated with the increased light attenuation, both through the direct shading effect of suspended sediments and through the promotion of phytoplankton and epiphyte growth by the associated increase in nutrients (Terrados et al., 1998; Halun et al., 2002; Brodersen et al., 2015). Therefore, the increase in seawater turbidity and considerable sediment redeposition on the leaves severely impaired the light availability and photosynthetic activity, as indicates LA/ALA > 1 in the above-ground tissue resulting from decreased conversion of LA to ALA (Harris and James, 1965). When minimum light requirements are not met (~14% of incidence light) the seagrass intensely sheds its leaves and shoots (Collier et al., 2012). Such light condition apparently persisted until May 2018 and most likely prevented the re-establishment of photosynthesis and C. nodosa continued to shed shoots and leaves. The reduced photosynthesis and therefore O_2 transport from the leaves to the rhizome-root system probably minimized root respiration. The maintenance of the oxic rhizosphere and the internal O_2 partial pressure in the lacunae further depended mainly on the diffusion of O_2 from the water column (Pedersen et al., 1998; Greve et al., 2003; Sand-Jensen et al., 2005). From April to June 2018, O_2 in the bottom water drastically decreased. Due to poor supply, O_2 content of below-ground tissue was too

low to maintain an oxic microenvironment and therefore, the plant tissues became potentially accessible to sulfide intrusion (Pedersen et al., 2004).

At the same time, the sediment was enriched with new organic matter derived from increased autotrophic biomass in bottom waters. In addition to the induction of the benthic bloom, strong sediment resuspension, most likely by aeration, stimulated the intense oxidation of H_2S that started to produce in the rooted zone (up to 180 μM). An increase in S^0 concentration that reached its maximum in the same layer suggests a simultaneous oxidation of the produced H_2S. The sulfide oxidation probably caused oxygen depletion in the rooted zone and anoxic zone extension up to the sediment subsurface. In May 2018, the excess of organic matter accumulated in April 2018 was degraded. The concentrations of S^0, detected only in the suboxic layer, considerably decreased possibly by disproportionation or respiration by members of the sulfate-reducing bacteria (Pjevac et al., 2014).

During June and July 2018, a sudden and significant deterioration of C. nodosa physiological condition was indicated by the further increase in LA/ALA ratio in the leaves and overall saturation of decreasing lipids in above- and below-ground tissues. Additionally, the loss of leaf tissue negatively impacted the photosynthetic carbon fixation (Lee and Dunton, 1997; Lee et al., 2007). The below-ground tissue that was not supported by photosynthetically derived oxygen became anoxic. Thus induced anaerobiosis most likely caused a complete inhibition of the fatty acid desaturation chain (Harris and James, 1965) and permanent breakdown of photosynthesis leading to the final decay of the aboveground biomass and considerable loss of below-ground biomass. In July 2018, the bottom waters were completely depleted in O_2 and the whole plant exposed to sulfides. H_2S inhibit cytochrome c oxidase by binding to regulatory sites on the enzyme, reducing the rate of cellular respiration and leading to the chemical asphyxiation of cells (Nicholls et al., 2013).

From June to August 2018, the decomposition of organic matter, encompassing the entire sediment core, was intensified and accompanied by a large increase in H_2S concentrations (up to 1200 μM). The degradation process involved rhizomes and roots, as suggested by an apparent loss of below-ground biomass. Such loss typically occurs in the first stage of plant decay, the leaching phase (Trevathan-Tackett et al., 2017). Readily available, soluble carbohydrates that largely contribute to leachate mass (Vichkovitten and Holmer, 2004) most probably supported the increase in prokaryotic abundance observed in June and July 2018, and also high rates of sulfate reduction. However, the significant decreases in PA that coincided with a maximum degradation of organic matter and H_2S production in August 2018 might indicate that remaining compounds were not degradable by the sulfate reduction pathway (Arndt et al., 2013) and needed the presence of prokaryotes specialized in the anaerobic degradation of refractory compounds, including cellulose and lignin.

During September and October 2018, due to the combined effect of freshened oxygenated water input and resuspension which gradually deepen the oxic layer, H_2S concentrations drastically decreased due to re-oxidation. Biogeochemical studies suggest most sulfide (80–90%) is eventually re-oxidized, while only 10–20% is ultimately buried as complexes with iron (i.e. FeS, FeS_2) or with organic matter after sulfurization (Jørgensen, 1977; 1982). H_2S scavenging with iron and formation of iron sulfides might be more critical in Saline Bay since terrestrial waters are washing out terra rossa, rich in Fe-oxides and oxyhydroxides (Durn, 2003). For this reason, sediment cores were most likely always black with sulfuric odor, irrespective of H_2S concentrations or presence of vegetation.

COMMENT: Decreased root respiration may also contribute to the dying off

RESPONSE: *We agree that the decreased root respiration contributed to C. nodosa dying off. We believe that reduced O_2 transport from the leaves to the rhizome-root system minimized or even stopped root respiration. Moreover, the lack of sediment oxygenation compromised the metabolic activities of aerobic bacteria around the roots and their oxidation of H_2S. A commentary regarding root respiration was added within the re-arranged Discussion.*

CHANGE (Page 21, Line 635 – 637): *The reduced photosynthesis and therefore O_2 transport from the leaves to the rhizome-root system probably minimized root respiration*

COMMENT: Changes of unsaturated fatty acids could be attributed to many sources, since phytoplankton or microalgae are the main producers of these compounds, it is hard to guess.

RESPONSE: *We are aware that changes in unsaturated fatty acids could be attributed to many sources. Particularly in the sediment their changes depend on the dynamic interactions between primary producers and their consumers within the food web. In this paper, the intention was to compare vegetated and control (non-vegetated) sediment using different markers and indices which together provided an indicative interpretation of the predictable sources. More complex analysis of the sources exceeds the scope of this paper and will be the topic of further investigation.*

COMMENT: While grazing rate might be responsible for the changes in seasonal change of stand crop of the seagrass, the authors did not provide any record that grazing rate is higher in the Saline Bay.

RESPONSE: *In July and August 2017 the leaves were very short with visible signs of bites, so we assumed that lower biomass and leaf length in these two months were the result of grazing activity of herbivores. In addition, in a nearby bay where we performed biometric measurements in C. nodosa meadow simultaneously, we did not notice such intense leaves damage and the vast majority of leaves had intact apexes. We rephrased the sentences to avoid misleading interpretation and have added the references that support biomass loss by herbivory in C. nodosa.*

CHANGE (Page 17, Lines 501 – 504): *In Saline Bay, the maximum biomass was measured in October 2017. This shift from summer to early autumn was most likely due to an intense*

grazing activities (Cebrian et al., 1996; Valentine and Duffy, 2006) suggested by a prevalence of visibly grazed leaves during July and August.

COMMENT: During summer period, high light and temperature may synergistically reduce the biomass of the seagrass due to higher respiration and higher photoinhibition.

RESPONSE: We are aware of this synergistic effect of high light and high temperature on the reduction of biomass related to seagrasses growing near or within the intertidal zone where they may be exposed to high light stress which may then result in down-regulation of photosynthetic apparatus or if irradiance is too high by photoinhibition. As the sampling depth in Saline Bay (3 - 4 m) was not in the intertidal region and tidal oscillation does not exceed 50 cm, we believe that this mechanism did not contribute to the reduction of C. nodosa biomass either in summer 2017 or in summer 2018. The biomass reduction and meadow die-off started when the temperature were still moderate. When the temperature reached its maximum (August 2018) the meadow had already died and therefore, the effect of the high temperature could not be displayed.

COMMENT: Repeated wordings should be avoided in a sentence or paragraph.

RESPONSE: This was considerably avoided by rearranging the Discussion, otherwise checked and corrected accordingly throughout the text.

COMMENT: Unit of silicate should be double checked, might be mistaken

RESPONSE: The unit of silicate was double checked. Silicates (orthosilicates or reactive silicates) were determined spectrophotometrically by molybdenum blue method. Calibration was performed in the range $0.5 – 20 \mu mol\ L^{-1}$ of sodium silicofluoride, Na_2SiF_6. Accordingly, the results were presented in $\mu mol\ L^{-1}$ (μM).

COMMENT: Line 83 change shorter to shorten…*changed (Line 88)*

1   Dynamics of environmental conditions during a decline of a *Cymodocea nodosa* meadow

2

3   Mirjana Najdek[1], Marino Korlević[1], Paolo Paliaga[2], Marsej Markovski[1], Ingrid Ivančić[1],

4   Ljiljana Iveša[1], Igor Felja[3] and Gerhard J. Herndl[4,5]

5   [1]Center for Marine Research, Ruđer Bošković Institute, G. Paliaga 5, 52210 Rovinj, Croatia

6   [2]Department of Natural and Health Sciences, University of Pula, Zagrebačka 30, 52100 Pula,

7   Croatia

8   [3]Department of Geology, Faculty of Science, University of Zagreb, Horvatovac 102a, 10000

9   Zagreb, Croatia

10   [4]Limnology and Bio-Oceanography, Center of Functional Ecology, University of Vienna,

11   Althanstrasse 14, 1090 Vienna, Austria

12   [5]NIOZ, Department of Marine Microbiology and Biogeochemistry, Royal Netherlands

13   Institute for Sea Research, Utrecht University, PO Box 59, Alberta, Den Burg, 1790, The

14   Netherlands

15   *Correspondence to*: Mirjana Najdek (najdek@cim.irb.hr)

Abstract. The dynamics of the physicochemical and biological parameters were followed during the decline of a *Cymodocea nodosa* meadow in the northern Adriatic Sea from July 2017 to October 2018. During the regular growth of *C. nodosa* from July 2017 to March 2018, *C. nodosa* successfully adapted to the changes of environmental conditions and prevented H_2S accumulation by its re-oxidation, supplying the sediment with O_2 from the water column and/or leaf photosynthesis. ~~The *C. nodosa* decline was most likely triggered in April 2018 by a reduction of light availability which affected photosynthesis of C. nodosa and the oxidation capability of below-ground tissue.~~ The *C. nodosa* decline was most likely triggered in April 2018 when light availability to the plant was drastically reduced due to increased seawater turbidity that resulted from increased terrigenous input combined with resuspension of sediment and elevated autotrophic biomass. Light reduction impaired photosynthesis of *C. nodosa* and the oxidation capability of below-ground tissue. Simultaneously, a depletion of oxygen due to intense oxidation of H_2S occurred in the sediment, thus creating anoxic conditions in most of the rooted areas. These linked negative effects on the plant performance caused an accumulation of H_2S in the sediments of the *C. nodosa* meadow. During the decay of above- and below-ground tissues, culminating in August 2018, high concentrations of H_2S were reached and accumulated in the sediment as well as in bottom waters. The influx of oxygenated waters in September 2018 led to the re-establishment of H_2S oxidation in the sediment and ~~recovery~~ remaining of the below-ground tissue. Our results indicate that if disturbance of environmental conditions, particularly those compromising the light availability, takes place during the recruitment phase of plant growth when metabolic needs are at maximum and stored reserves minimal, a sudden and drastic decline of the seagrass meadow occurs.

1 Introduction

Seagrasses are important ecosystem engineers constructing valuable coastal habitats which play a key role in the preservation of marine biodiversity and carbon sequestration (Duarte et al., 2013; Samper-Villareal et al., 2016). Seagrasses extend their active metabolic surfaces (i.e., leaves, rhizomes and roots) into the water column and in the sediment, where root activity might modify the chemical conditions (Marbà and Duarte, 2001). Their canopies and dense meadows are responsible for trapping substantial amounts of sediment particles and organic matter, enhancing water transparency and sediment stability with the dense network formed by the rhizome (Gacia and Duarte, 2001; Hendriks et al., 2008; Widdows et al., 2008). Seagrass rhizospheres store organic matter (Pedersen et al., 1997), promote sulfate reduction (Holmer and Nielsen, 1997), release oxygen (Pedersen et al., 1998) and alter sediment redox potential.

Seagrasses require some of the highest light levels of any plant worldwide to provide oxygen to roots and rhizomes and support a large amount of non-photosynthetic tissue (Orth et al., 2006). This make seagrasses sensitive to environmental changes, especially those that deteriorate light availability, such as sediment loading, eutrophication or epiphyte cover on seagrass leaves (Terrados et al., 1998; Halun et al., 2002; Brodersen et al., 2015; Costa et al., 2015). Seagrasses have adapted to a highly variable light environment providing tolerance to short-term periods of low light conditions by balancing carbon supply and respiratory requirements. In a healthy growing population this balance is achieved by increasing the photosynthetic activity, re-allocation of carbohydrate reserves from rhizomes and slowing down growth rates (Collier et al., 2009). Beside metabolic and physiological changes, stress responses under poor light conditions include shedding of leaves and shoots and production of new, altered tissue. At sub-lethal light levels, these changes may be permanent. Below these species-specific minimum light requirements seagrass populations are dying off (Collier et al., 2012). Membrane lipids, particularly polyunsaturated fatty acids (PUFA), as the most responsive constituents have a major role in the adaptation processes of primary producers to fluctuating environmental factors, such as temperature, irradiance or salinity (Viso et al., 1993; Lee et al., 2007; Schmid et al., 2014; Sousa et al., 2017; Beca-Carretero et al., 2018; Beca-Carretero et al., 2019). The changes in the unsaturation degree (UND) of membrane fatty acids affect the maintenance of membrane functions and its resistance to cold stress or

poor light conditions. UND depends mostly on the variation of α-linolenic (C18:3n-3, ALA) and linoleic (C18:2n-6, LA), the major unsaturated fatty acids in leaves, implicated in the evolution of oxygen during photosynthesis. LA and ALA are derived from oleic acid by desaturation in the chloroplast and this conversion considerably declines in the dark, being completely inhibited by anaerobiosis (Harris and James, 1965).

Sediments inhabited by seagrasses are usually anoxic, highly reduced and rich in sulfide (H_2S), a strong phytotoxin (Koch and Erskine, 2001) which has been implicated in several die-off events of seagrasses (Carlson et al., 1994; Borum et al., 2005; Krause-Jensen et al., 2011). H_2S is produced by sulfate-reducing bacteria that use sulfate as a terminal electron acceptor for the mineralization of organic matter (Jørgensen, 1977; Capone and Kiene, 1988, Canfield et al., 1993). High H_2S concentrations may occur as a consequence of enhanced mineralization due to increased temperature, organic loading or oxygen depletion (Moeslund et al., 1994; Pérez et al., 2007; Mascaró et al., 2009). Under these conditions, sulfides may intrude into plant. Re-oxidation of H_2S in the rhizosphere by incorporation of S^0 in the below-ground tissue has been recognized as a major survival strategy of seagrasses in sulfidic sediments (Pedersen et al., 2004; Holmer et al., 2005; Hasler-Sheetal and Holmer, 2015). Generally, the synergistic effect of oxygen depletion and other stresses, such as sulfide toxicity may shorten the survival of benthic communities and possibly accelerate mortality events (Vaquer-Sunyer and Duarte, 2010).

The seagrass *Cymodocea nodosa* (Ucria) Ascherson is widely distributed and common species throughout the Mediterranean (Terrados and Ros 1992; Pedersen et al., 1997; Cancemi et al., 2002; Agostini et al., 2003). For the northern Adriatic, however, only sparse data are available on the standing crop, seasonal dynamics or natural/anthropogenic pressures supporting the ecological or conservation status of *C. nodosa* meadows (Zavodnik et al., 1998; Orlando-Bonaca et al., 2015; 2016). Although *C. nodosa* show large phenotypic plasticity adapting to diverse natural and anthropogenic stressors by physiological and morphological adaptations, a severe decline has been reported during the last decades in coastal areas (Orth et al., 2006; Short et al., 2011; Tuya et al., 2002; 2014), including the northern Adriatic (Orlando-Bonaca et al., 2015; 2019). One of these declines was documented in our study performed from July 2017 to October 2018 in Saline Bay (northern Adriatic Sea). A series of monthly physicochemical and biological measurements were conducted in *C. nodosa* tissues, sediment underlying the *C. nodosa* meadow, non-vegetated sediments and

103 surrounding water to i) determine the link between ambient seawater and sediment

104 environmental factors influencing the growth of *C. nodosa*, ii) document the response of *C.*

105 *nodosa* to the changes in environmental conditions that led to the meadow decline and iii)

106 evaluate the conditions leading to the decline of *C. nodosa*.

107 **2 Materials and methods**

108 2.1 Study site

109 Saline Bay is located 4 km northwest of Rovinj (Croatia) at the coast of the northern Adriatic

110 Sea (45°7′5″N; 13°37′20″E, Fig. S1). The bay represents the terminal shallow part of an 800

111 m long inlet, open towards the northwest. The southeastern coast of Saline Bay is

112 characterized by relatively pristine conditions, while the northwestern littoral part has been

113 completely modified by the excavation of coastal mud and the addition of large amounts of

114 gravel to create an artificial beach. Large amounts of silty red soil (*terra rossa*) can be found

115 in the south eastern inner part of the bay in a large muddy flatland which is slowly being

116 eroded by the sea and rain weathering. The main input of freshwater to the bay represents land

117 drainage canals since the year 2017. Even though Saline Bay is protected from the prevailing

118 winds (from the NE and SE) circulations from the northwestern quadrant can occasionally

119 trigger bigger waves resuspending the surface sediments and giving the waters a muddy

120 appearance. At the beginning of this study, the seafloor was covered with large *C. nodosa*

121 meadows spreading from the southwestern coastal area (1.5 m depth) toward the central part

122 of the bay (4 m depth), while at the end of the study only a few small patches persisted in tiny

123 stripes along the shoreline.

124

125 2.2 Sampling

126 The sampling was performed for 15 months from July 2017 to October 2018. Seawater for

127 analyses of nutrients, chlorophyll a (Chl *a*), particulate matter concentration and prokaryotic

128 abundance was sampled using plastic containers (10 L). *C. nodosa* (3 – 4 m of depth) was

129 collected together with rhizomes, roots and epiphytic macroalgae by divers using the quadrat

130 sampling method. Three quadrats (20 x 20 cm) were randomly scattered in positions of

131 maximum seagrass coverage (e.g. 100 %). Sediment samples were collected inside vegetated

132 and non-vegetated sediment by divers using plastic core samplers (15 cm, 15.9 cm^2). For

133 granulometric composition, organic matter, prokaryotic abundance, total lipids and fatty acid

134 analyses, the cores were cut into 1 cm sections to a depth of 8 cm and lyophilized, except of

135   sections for prokaryotic abundance analysis, that were weighted (approx. 2 g) and fixed with

136   formaldehyde (final conc. 4% v/v) immediately after slicing the sediment core.

137

138   2.3 Temperature (T) and salinity (S) measurements

139   T was measured continuously (in 30 min. intervals) using HOBO pendant temp/light Data

140   Loggers (Onset, USA) which were replaced at each sampling. S was measured on sampling

141   dates by a pIONneer 65 probe (Radiometer analytical, Copenhagen).

142

143   2.4 Inorganic nutrients, Chl *a* and particulate matter (PM) analysis

144   Seawater for all analysis was filtered through combusted Whatman GF/F filters. Nitrate

145   (NO_3), nitrite (NO_2), ammonia (NH_4), phosphate (PO_4) and silicate (SiO_4) were analyzed

146   spectrophotometrically according to Strickland and Parsons (1972). Chl *a* was determined on

147   filters by the fluorometric procedure after extraction in 90 % acetone (Holm-Hansen et al.,

148   1965). PM was determined gravimetrically after filtering up to 5L seawater on pre-weighed,

149   filters which were dried (at 60°C) and reweighed.

150

151   2.5 Determining prokaryotic abundance

152   For determining the prokaryotic abundance in seawater, 2 ml of formaldehyde (final conc. 4%

153   v/v) fixed samples were stained with 4,6-diamidino-2-phenylindol (DAPI, 1 µg mL^{-1} final

154   conc.) for 10 min (Porter and Feig, 1980). In sediment samples, prokaryotes were detached

155   from the sediment particles by addition of Tween 80 (0.05 mL) and ultrasonicated for 15 min

156   (Epstein and Rossel, 1995). After sonication, 1 mL of the supernatant was stained with DAPI

157   (final conc. 5 µg/mL). DAPI stained samples were filtered onto black polycarbonate filters

158   (Whatman, Nuclepore, 0.22 µm) and counted under an epifluorescence microscope (Zeiss

159   Axio Imager Z1).

160

161   2.6 Biometry of *C. nodosa* and epiphytic macroalgae

162   The material from each quadrat was washed under running seawater to remove sediment.

163   From each quadrat algae, leaves and rhizomes with roots were separated. The length of the

164   longest leaf on each shoot was measured and the shoots were counted. Species of macroalgae

165   were determined, and their coverage was estimated according to the Braun-Blanquet scale.

166   Separated samples were washed with filtered and autoclaved seawater, weighed, dried at 60

167   °C for 48 h and re-weighed. The dry mass was calculated per area (g m^{-2}).

168

169   2.7 Granulometric composition of the sediment and its organic matter content

170   For granulometric analysis of the sediment, each sample was wet sieved through a set of

171   seven standard ASTM sieves (4-, 2-, 1-, 0.5-, 0.25-, 0.125-, 0.063-mm mesh size). The

172   fraction that passed through the 0.063-mm sieve was collected and analyzed following the

173   standard sedigraph procedure (Micromeritics, 2002). The material that was retained on the

174   sieves was dried and weighted. The data obtained by both techniques were merged to obtain a

175   continuous grain size range and analyzed with the statistic package Gradistat v 6.0. Sediments

176   were classified according to Folk (1954). The sediment permeability was calculated based on

177   median grain size (d_g) following the empirical relation by Gangi (1985). The organic matter

178   content was determined as ignition loss after heating dried sediment sections at 450°C for 4 h

179   in a muffle furnace.

180

181   2.8 Oxygen (O_2), hydrogen sulfide (H_2S) and redox potential (Eh) profiling

182   The microprofiles of O_2, H_2S and Eh were measured on intact cores immediately after

183   sampling using a motorized micromanipulator (MMS9083) equipped with microsensors OX-

184   100 and H_2S-200, redox microelectrode RD-200 coupled with reference electrode REF-RM

185   (Unisense A/S, Denmark). Prior to the measurements, the OX-100 microsensor was calibrated

186   using a two-point oxic – anoxic calibration; H_2S-200 was calibrated in fresh Na_2S solutions

187   using eight-point calibration (1μM - 300 μM in a de-oxygenated calibration buffer

188   (NaAc/HAc, pH <4); RD-200 with REF-RM was calibrated using two point calibration by

189   simultaneous immersion of electrodes in quinhydrone redox buffers prepared in pH 4 and pH

190   7 buffers, all according to the manufacturer's recommendation. During measurements,

191   sediment cores were placed in a pool filled with seawater from the sampling site to maintain

192   *in situ* temperature. From July to October 2017 H_2S was measured spectrophotometrically in

193   pore waters (Cline, 1969) squeezed out by centrifugation from each section (5 mm) of the

194   sediment cores.

195

196   2.9 Total lipids, fatty acid composition and elemental sulfur (S^0)

7

197   Lyophilized samples of seagrass tissues, macroalgae, sediment or particulate matter were

198   weighed and extracted into a solvent mixture of dichloromethane/methanol (DCM: MeOH,

199   2:1) in an ultrasonic bath at 35°C with three solvent mixture changes. The extracts were

200   pooled and separated into layers by addition of 0.9% NaCl solution. Lower DCM layers

201   (containing lipids) were released over Na_2SO_4 anhydride, collected in pre-weighed round

202   bottom flasks and evaporated to dryness using rotavapor. After evaporation, flasks were re-

203   weighed, and total lipid concentrations (TL, mg g^{-1} DW) were calculated from the difference

204   in weight. For fatty acids determination, lipid extracts were saponified (1.2 M NaOH in

205   methanol), acidified (6 M HCl), methylated (14% BF_3 in methanol) and extracted into DCM.

206   Fatty acid methyl esters (FAME) were analyzed by Agilent gas–liquid chromatography

207   (GLC) 6890 N GC System equipped with a 5973 Network Mass Selective Detector, capillary

208   column (30 m x 0.3 mm x 0.25 µm; cross-linked 5 % phenylmethylsiloxane) and ultra-high

209   purity helium as the carrier gas. The GLC settings were as follows: programmed column

210   temperature rise from 145°C by 4°C/min to 215°C, then by 1°C/min to 225°C and finally by

211   4°C/min to 270°C at constant column pressure of 2.17 kPa. Retention times, peak areas and

212   mass spectra were recorded on the ChemStation Software. FAME were identified by mass

213   spectral data and family plots of an equivalent chain length (ECL) for GC standards. Applied

214   GC standards were: FAME mix C18–C20, PUFA1, PUFA3 standards (Supelco/Sigma-

215   Aldrich, Bellefonte, PA, USA); C4–C24 FAME standard mix, cod liver oil and various

216   individual pure standards (Sigma, Neustadt, Germany).

217   The following indices of fatty acid profiles were calculated: saturated fatty acids (SAT),

218   monounsaturated fatty acids (MUFA), polyunsaturated fatty acids (PUFA) and the

219   unsaturation degree (UND). UND was employed to evaluate the degree of organic matter

220   degradation due to more susceptibility of unsaturated, particularly polyunsaturated,

221   components to degradation and calculated according to the formula

222   [1*(% mono-)+2*(% di-)+3* (% tri-)+4*(% tetra-)+5*(% penta-)+6*(% hexa-enoic)]/% SAT

223   (Pirini et al., 2007). To evaluate the input of terrestrial organic matter relative to that of

224   marine origin in particulate matter, the terrestrial to aquatic acid ratio (TAR= C24+C26+C28 /

225   C12+C14+C16) was used (Cranwell et al., 1987; Bourbonniere and Meyers, 1996).

226   In FAME chromatograms elemental sulfur (S^0), eluted as S_8 (m/z 256), was identified by

227   comparison of retention time and characteristic fragment ions in samples and standard

228   solutions. The concentration of S^0 was estimated on the base of the calibration curve prepared

229 for standard solution of S_8 (Aldrich, Germany) in cyclohexane (2-20 mg L^{-1}). The calibration

230 curve was determined under the same GLC settings as FAME. Limit of detection (LoD) and

231 limit of quantitation (LoQ) were calculated from the parameters of the calibration curve

232 constructed on the basis of the 3 lowest concentrations in 3 replicates. LoD and LoQ (0.92 mg

233 L^{-1} and 2.80 mg L^{-1}, respectively) were more than twice the values obtained by Rogowska et

234 al. (2016) probably due to higher injector and column temperature used in this study than they

235 proposed as optimal for S determination.

236

237 2.10 Data analyses

238 A multivariate analysis, hierarchical clustering and K-means methods (Systat 12) was applied

239 to group *C. nodosa* above- and below-ground tissues according to the similarity of their fatty

240 acid profiles and indices, i.e., physiological condition during the investigated period.

241   Sediment data were analyzed for two groups of sediment layers, the upper layer (0- 4 cm)

242 where most of rhizomes and roots are located, and the lower layers (5-7 cm). Differences

243 between vegetated and non-vegetated sediment samples in each sediment layer were tested by

244 one-way ANOVA. Correlations among parameters were tested using the Pearson's correlation

245 coefficient (r). The level of statistical significance was $p < 0.05$. A multivariate principal

246 component analysis (PCA, Primer 6) was applied to identify the most important variables

247 explaining differences between vegetated and non-vegetated sediments. Correlation matrices

248 were constructed using variables: H_2S, Eh, O_2, S^0, PA, TL and UND. All variables were

249 normalized due to their different scales. Only the principal components with eigenvalues >1

250 were considered.

251

252 **3 Results**

253 3.1 Water column

254 3.1.1 Environmental variables

255 During summer of 2017 daily means of sea-bottom temperature in *C. nodosa* meadow ranged

256 between 26°C and 28°C. During autumn seawater temperatures decreased below 12°C until

257 the end of December. The coldest period was recorded at the beginning of March lasting only

258 for a few days (min. 8.62°C). From April to mid-July 2018, temperature increased with

259 moderate fluctuations to the maximum of 29.26°C recorded in August 2018 (Fig. 1a).

260   Concentrations of inorganic nutrients and Chl *a* were generally low. The highest

261   concentrations (DIN: 8.27 µM; PO$_4$: 0.18 µM; SiO$_4$: 9.82 µM; Chl *a*: 0.89 µg L^{-1}) associated

262   with the lowest salinity (34.2) were found in September 2017 (Table S1). The abundance of

263   prokaryotes (2.6-11.3 x 10^5 cell mL^{-1}) varied seasonally and significantly correlated to

264   seawater temperatures (r = 0.618; p < 0.05). In contrast, salinity (S: 34.2 - 38.5) and

265   concentrations of particulate matter (PM: 3.84 - 14.21 mg L^{-1}) showed irregular variations

266   (Fig. 1b) and a significant opposite trend (r = -0.630; p < 0.05).

267   The particulate lipids exhibited the highest unsaturation degree (UND) during

268   summer/early autumn 2017 and small increases of UND in April and September/October

269   2018 (Fig. 1c). UND was significantly correlated with Chl *a* (r = 0.603; p < 0.05). In contrast,

270   terrestrial to aquatic ratio (TAR) considerably increased in April and was the highest in

271   August 2018 (Fig. 1c). TAR was negatively correlated to UND (r = -0.644, p < 0.05) and

272   positively to particulate matter (r = 0.641, p < 0.05). Although PUFA with 18 C atoms made

273   the largest contribution to the total PUFA pool, C20 PUFA, mainly of phytoplankton origin,

274   showed a similar trend as observed for UND (Fig. S2, Table S2).

275

276   3.2 *Cymodocea nodosa* meadow

277   3.2.1 Biometry

278   *C. nodosa* leaves and shoots reached the highest biomass (285.3 ± 57.4 g m^{-2}), length (102.4 ±

279   26.6 mm) and shoot density (3703±334 shoots m^{-2}) in October 2017 (Fig. 2a). After the

280   appearance of the regular vegetation minimum in November 2017, biometric indices further

281   decreased reflecting the decay of the meadow in summer 2018. In August 2018, only yellow

282   to brownish leaves on sparse shoots were collected (4.5 ± 1.3 g m^{-2}, 5.4 ± 1.3 mm and 30 ± 35

283   shoots m^{-2}). In September and October 2018, no shoots or leaves were observed (Fig. 2a). The

284   biomass of rhizomes and roots reached also its maximum in October 2017 (599.7 ± 36.8 g m^{-2}

285   ^{2}). In contrast to leaves and shoots, the belowground biomass was stable until March 2018

286   when a decline was observed that continued until October 2018 (30.5 ± 6.8 g m^{-2}) (Fig. 2a).

287

288   3.2.2 Total lipid (TL) concentrations and fatty acid composition

289   TL in the *C. nodosa* above-ground tissue (6.7 - 25.3 ± 2.4 mg g^{-1} DW) increased until

290   February 2018, when maximum TL concentrations were measured (Fig. 2b). Thereafter, TL

291   concentrations decreased until August 2018. During this period, the belowground TL

292 concentration (6.3 ± 1.9 – 15.9 ± 1.1 mg g^{-1} DW) was generally lower than the above-ground

293 TL concentrations and the trend was similar to that of leaves. The minimum concentrations of

294 TL were observed in September 2018, while in October 2018, concentrations similar to that

295 measured in October 2017 were observed (Fig. 2b).

296   The major fatty acid components in *C. nodosa* tissues were palmitic (C16:0) amongst the

297 saturated (SAT) and oleic (C18:1n-9) in monounsaturated fatty acids (MUFA). In the above-

298 ground tissue, the main polyunsaturated fatty acids (PUFA) were α-linolenic (C18:3 n-3,

299 ALA) and linoleic (C18:2 n-6, LA), while in the belowground tissue LA was dominant (Fig.

300 2b). The dynamics of UND in the above-ground tissue was principally influenced by changes

301 in ALA and LA. LA/ALA ratios were < 1 from July 2017 to March 2018, and > 1 from April

302 to July 2018 (Fig. 2b). In August 2018, the LA/ALA ratio was infinite due to the absence of

303 ALA (Fig. 2b). Elemental sulfur (S^0) was detected only in decaying leaves in August 2018

304 (0.21 mg g^{-1} DW). In the belowground tissue, S^0 was detected in all samples (Fig. 2b). Higher

305 concentrations were measured during summer 2017 (up to 0.39 ± 0.06 mg g^{-1} DW). S^0

306 increased from minimum concentrations in April (0.02 ± 0.01 mg g^{-1} DW) until September

307 2018 reaching 1.42 mg g^{-1} DW (Fig. 2b).

308   According to the fatty acid profiles, *C. nodosa* leaves were classified in three groups,

309 except for the leaves collected in August 2018 (Fig. 3). The most distinguishing features

310 specifying physiological differences between Group 1 (July - October 2017 and February -

311 March 2018), Group 2 (November - December 2017 and April - May 2018) and Group 3

312 (June and July 2018) were decreasing mean values of PUFA, UND, ALA and LA and

313 increasing means of SAT and the proportion of long-chain saturated fatty acids (C ≥ 24). In

314 the ungrouped leaves from August 2018 ALA was not found, PUFA and UND were at a

315 minimum, while SAT and C ≥ 24 at a maximum (Table S3). Three groups of rhizomes and

316 roots (Group 1: July - October 2017 and February - March 2018; Group 2: November -

317 December 2017 and April - May 2018 and Group 3: (June - October 2018) showed similar

318 characteristics to the groups 1, 2 and 3 of related leaves (Table S4).

319

320 3.2.3 Epiphytic macroalgae

321 From July 2017 to February 2018 different taxa of macroalgae belonging to the three phyla

322 Chlorophyta (*Halimeda tuna*, *Dasycladus vermicularis*, *Cladophora prolifera*, *Udotea*

323 *petiolata*), Rhodophyta (*Rytiphlaea tinctoria*, *Peyssonnelia* spp, *Gelidium* sp.) and

324 Ochrophyta (*Dictyota dichotoma*) were covering the meadow in varying proportions and

325 abundances (Fig. 4). After March 2018, when only few individuals of *Peyssonnelia* sp. were

326 found, macroalgae were no longer present in the *C. nodosa* meadow.

327 Although the fatty acid profiles of macroalgal communities were highly variable, the

328 contribution of 18- and 20 PUFA to the total PUFA pool generally depended on the prevailing

329 phyla and their characteristic PUFA pattern. The algae belonging to Rhodophyta and

330 Ochrophyta are richer in 20 PUFA (C20:5n-3, C20:4n-6), while Chlorophyta are generally

331 showing prevalence of 18 PUFA (C18:3n-3, C18:2n-6) (Schmid et al., 2014, Gao et al.,

332 2018). Furthermore, their contribution to biomass varied due to large differences in

333 morphology, which most likely also contributed to the variability of fatty acid profiles. 18

334 PUFA and 20 PUFA showed the highest contribution to the total PUFA pool during the

335 dominance of Chlorophyta and Rhodophyta in the macroalgal community, respectively. In

336 most samples, the lowest contribution to the total PUFA pool was observed for 16 PUFA and

337 22 PUFA (Fig. S3).

338

339 3.3 Sediment

340 3.3.1 Granulometric composition

341 According to the granulometric composition, median grain sizes (d_g) and permeability (k) the

342 vegetated and non-vegetated sediments were classified as slightly gravelly sandy mud (g)sM,

343 fine grained ($d_g < 165$ µm) and low permeable to impermeable sediment ($k < 2 \cdot 10^{-11}$ m^2). In

344 general, the *C. nodosa* sediment consisted of a significantly higher proportion of sand (Sa),

345 and lower proportion of silt (Si) and clay (C) (Sa, 41.11 ± 4.34 %; Si, 46.44 ± 2.86 %; C, 9.63

346 ± 2.76 %) in comparison to non-vegetated sediment (Sa, 20.53 ± 10.49 %; Si, 53.24 ± 6.76 %;

347 C, 23.29 ± 4.86 %). The median grain size and permeability in *C. nodosa* sediment (d_g, 37.51

348 ± 17.97 µm, k, $1.22 \cdot 10^{-12} \pm 1.13 \cdot 10^{-12}$ m^2) were significantly higher than in non-vegetated

349 sediment (d_g, 10.86 ± 5.34 µm; k, $1.04 \cdot 10^{-13} \pm 1.02 \cdot 10^{-13}$ m^2). The upper layers of both cores

350 (0 - 4 cm) had larger particles, while the lower layers (5 - 8 cm) showed a uniform distribution

351 of smaller grain sizes (Fig. 5).

352

353 3.3.2 O$_2$, E$_h$, H$_2$S and S^0

354 Oxygen concentrations (O$_2$) in the bottom water of the *C. nodosa* meadow varied in a wide

355 range (0 µM - 171.4 ± 17.6 µM) and generally followed the O$_2$ saturation trend (Fig. 6a).

356   From May to June 2018, O_2 decreased below 62.5 μM, considered as severe hypoxia (Vaquer-

357   Sunyer and Duarte 2008) and was completely depleted in July 2018 (Fig. 6a). From August to

358   October 2018, O_2 increased again. The variations of O_2 in the bottom water of the non-

359   vegetated sediment were similar to those in the *C. nodosa* meadow albeit generally higher

360   (79.4 ± 10.4 μM − 212.2 ± 33.4 μM) than in the vegetated sediment except for September and

361   October 2018 (Fig. 6a).

362   In general, O_2 penetration depth in the vegetated and non-vegetated sediment co-varied

363   with the O_2 concentration in the bottom layer, penetrating deeper when its concentration in the

364   bottom water was higher (Fig. 6b). In the vegetated sediment, O_2 was mainly depleted down

365   to 1 cm of depth. In the non-vegetated sediment, the oxygen penetration depth was up to 4

366   times higher than in vegetated sediments, except for the period from August 2018 to October

367   2018 when the penetration depths were similar (Fig. 6b).

368   The thickness of the oxic (Eh > 150 mV) and suboxic (150 mV > Eh > 0 mV) layers in the

369   vegetated sediment increased from July 2017 (~ 0.5 cm) to March 2018 (~ 4 cm), and

370   decreased progressively from April (~ 0.8 cm) towards the surface in July 2018, when the

371   entire sediment core was anoxic (Eh < 0). From August (~ 1 cm) to October 2018 (~ 2.5 cm)

372   the oxic and suboxic layer thickness increased again (Fig. 7). Oxic conditions (Eh > 0)

373   generally reflected O_2 concentrations in the bottom waters. The dynamics of Eh in non-

374   vegetated sediment were similar to those in the vegetated sediment. However, the thickness of

375   the oxic layer was considerably larger than in the vegetated sediment. Reducing conditions

376   (Eh < 0) were only recorded in July and August 2017 (Fig. 7).

377   Concentrations of free H_2S in the pore water of the vegetated sediment generally increased

378   with depth creating an accumulation zone mainly within the upper sediment layers (1 - 4 cm)

379   (Fig. 7). From July to November 2017, H_2S concentrations increased up to 120 μM (at 4 - 5

380   cm). In December 2017, H_2S was low and uniformly distributed throughout the core (< 5

381   μM). H_2S concentrations increased and the accumulation layer was ascending from March (up

382   to 34.2 ± 12.8 μM; 5 - 7 cm) to April 2018 (up to 177.2 ± 125.1 μM; 3.5 - 4.5 cm). During

383   May 2018 (up to 107.8 ± 75.9 μM; 2.5 - 4 cm), June (up to199.0 ± 6.3 μM; 1.5 - 6 cm) and

384   July (up to 210.1 ± 138.9 μM; bottom water - 6 cm) a propagation of the accumulation zone

385   was observed in addition to an increase in H_2S (Fig. 7). In August 2018 (up to 1164.1 ± 702.1

386   μM; bottom water - 7 cm) extremely high concentrations over the entire sediment core were

387   recorded. In September and October 2018, H_2S concentrations decreased (down to 140.0 ±

388 25.3 and 72.7 ± 52.7 µM; bottom water - 7 cm and 1 - 7 cm, respectively). In the non-

389 vegetated sediment, H_2S depth profiles were similar to those in vegetated sediments, but the

390 concentrations were generally lower, except for the summer of 2017 when the concentrations

391 were comparable but the accumulation zones deeper (Fig. 7).

392 S^0 mainly occurred in oxic (Eh > 150 mV) and suboxic (150 mV > Eh > 0 mV) layers of

393 both, vegetated and non-vegetated sediments (Fig. 7). Generally, the ranges of approximated

394 S^0 concentrations in vegetated sediment ($8.5 \cdot 10^{-5}$ - 0.39 mg·g^{-1} DW ~ $2.6 \cdot 10^{-3}$ - 12.1 µmol·g^{-1}

395 DW), except for the extreme value in April 2018 (0.99 mg·g^{-1} DW ~ 30.8 µmol·g^{-1} DW),

396 were similar to those found at the non-vegetated sites ($2.9 \cdot 10^{-4}$ – 0.28 mg·g^{-1} DW ~ $9.2 \cdot 10^{-3}$ –

397 8.9 µmol·g^{-1} DW).

398

399 3.3.3 Prokaryotic abundance

400 Prokaryotic abundance varied largely in vegetated (2.1 - 39.9· 10^7 cells g^{-1} fresh weight, FW)

401 and non-vegetated sediments (3.7 - 24.1·10^7 cells g^{-1} FW). Prokaryotic abundance was

402 significantly higher in the upper than the lower layers of vegetated (F = 40.553, p < 0.05) and

403 non-vegetated (F = 52.531, p < 0.05) sediments (Fig. 8). Prokaryotic abundance showed

404 significant monthly changes in the upper (F = 3.053, p < 0.05) and lower layer (F = 5.035, p <

405 0.05) of vegetated sediments, in contrast to both layers of non-vegetated sediments (p > 0.05).

406 Prokaryotic abundances were significantly higher in the upper layers (F = 44.577, p < 0.05)

407 and significantly lower in the lower layers (F = 5.986, p < 0.05) of vegetated than in the

408 respective layers of non-vegetated sediments (Fig. 8). In the upper sediment layer, prokaryotic

409 abundances were significantly higher in the vegetated than in the non-vegetated sediments

410 from July to October 2017 and from June to August 2018 (Fig. 8). In the lower layers of

411 vegetated sediments, prokaryotic abundance was significantly higher than in the non-

412 vegetated sediments in October 2017 and in August and September 2018 (Fig. 8).

413

414 3.3.4 Organic matter, total lipids and fatty acid composition

415 The concentrations of organic matter (OM) and total lipids (TL) were highly correlated in

416 vegetated (OM: 37.6 - 231.1 mg/g DW, TL: 0.15 - 2.75 mg/g DW; F = 214.172, p < 0.05) as

417 well as in non-vegetated sediments (OM: 56.7 - 160.3 mg/g DW, TL: 0.33 - 2.39 mg/g DW; F

418 = 45.569, p < 0.05). OM and TL generally decreased with depth and exhibited similar

changes throughout the investigated period with significantly higher concentrations in upper than in lower sediment layers ($p < 0.05$) (Fig. 9).

In the vegetated sediment, TL showed significant monthly changes in the upper ($F = 11.418$, $p < 0.05$) and lower sediment layers ($F = 3.186$, $p < 0.05$), in contrast to both layers of non-vegetated sediment ($p > 0.05$). From July to October 2017, in the upper layer of vegetated sediments, TL was significantly higher than in non-vegetated sediments (Fig. 9). From November 2017 onwards, TL decreased slightly until April 2018, reaching similar concentrations as TL in non-vegetated sediments (Fig. 9). TL concentrations decreased markedly in May and continued until August 2018. During that period, TL in vegetated sediments was significantly lower than in non-vegetated sediments. In September and October 2018, TL concentrations in vegetated sediments were similar to those in non-vegetated sediment (Fig. 9).

The fatty acid composition of vegetated and non-vegetated sediments was similar and in both layers characterized by the prevalence of SAT (vegetated upper: 71.2 - 90.4%, lower: 75.9-89.1%; non-vegetated upper: 71.2-80.7%, lower: 78.2-82.5%) over MUFA (vegetated upper: 7.6-22.9%, lower: 9.0-19.9%; non-vegetated upper: 17.8-24.1%, lower: 15.3-18.2%) and PUFA (vegetated upper: 1.9-6.9%, lower: 1.9-5.1%; non-vegetated upper: 1.7-4.8%, lower: 1.7-3.9%). The trends of the monthly changes in UND were similar in both layers of both sediment types. Those variations were less pronounced in the non-vegetated sediment where UND varied in narrower ranges in both layers (upper: 0.26-0.51, lower: 0.23-0.33) than in vegetated sediment (upper: 0.13-0.57, lower: 0.14-0.37). From July to October 2017 and in April 2018, UND was higher in the upper layers of vegetated sediment than in non-vegetated one, while from November 2017 to March 2018, UNDs of both sediments were lower than in previous period (Fig. 9). From June to August 2018, UND decreased considerably in vegetated sediment, being lower than in non-vegetated sediments. During September and October 2018, an increase of UND was observed in both sediments. In the lower layers, UNDs were similar, except for July and August 2018 when a considerable decrease of UND was observed in vegetated sediments (Fig. 9).

The proportions of PUFAs with chain lengths of 16, 18, 20, and 22 C atoms within the PUFA pool were similar between the respective layers of both sediments. Throughout the study period, the highest contribution of 18PUFA originated from *C. nodosa* detritus and Chlorophyta was observed (Fig. S4, Table S2). From July to October 2017, April to May

15

451   2018 and September to October 2018, a contribution of 20PUFA attributed to phytoplankton

452   and Rhodophyta was also detected. 16PUFA and 22PUFA accounted for the smallest

453   contribution to the PUFA pool and were found in seston and macroalgae (Fig. S4, Table S2).

454   The similarities between the sediments were also observed in the contribution of the main

455   SAT components to the SAT pool from July 2017 to March 2018 and from September to

456   October 2018 (Fig. S4, Table S2). From April to August 2018, an increase of the long-chain

457   (C$\geq$ 24) and common (C16:0 + C18:0) fatty acids followed by the decrease of bacterial fatty

458   acids (BACT) contribution to the SAT pool was observed in both layers of the vegetated

459   sediment. In contrast, the contribution of these components to the SAT pool was fairly

460   invariable in non-vegetated sediments during the same period (Fig. S4, Table S2).

461

462   3.3.5 Relationship between different physicochemical parameters

463   The relationships between H_2S, O_2, TL, S^0, PA, Eh and UND in vegetated and non-vegetated

464   sediment are shown in the principal component analysis, where PC1 explained 42.5 % and

465   PC2 14.4 % of variability (Fig. 10). The loadings for positive relationships were obtained for

466   H_2S (0.298) on PC1 and Eh (0.541) and O_2 (0.327) on PC2. For the negative relationships, the

467   loadings were for TL (-0.534), UND (-0.494), S^0 (-0.388), Eh (-0.327), PA (-0.296) and O_2 (-

468   0.191) on PC1, and H_2S (-0.536), S^0 (-0.485), TL (-0.165) and UND (-0.221) on PC2.

469   PC1 separated most of the upper sediment layers (July 2017 - May 2018, September -

470   October 2018) according to the higher concentrations of TL and S^0, higher UND and more

471   positive Eh from the most of the lower layers and upper layers of vegetated sediments (June -

472   August 2018) with increased H_2S concentrations. On PC2, the vegetated was separated from

473   the non-vegetated sediment due to higher concentrations of H_2S, S^0 and more negative Eh,

474   which characterized vegetated sediments during almost the entire study period. The extreme

475   concentrations of S^0 and H_2S found in the upper layer in April and the lower layer in August

476   2018, respectively, were responsible for the considerable separation of these layers from all

477   other vegetated layers (Fig. 10).

478

479   **4 Discussion**

480   Saline Bay is a shallow, highly dynamic coastal area characterized by frequent turbid waters

481   due to the combined effect of land run-off and wind-driven resuspension of fine sediment.

482   Nutrients and Chl a (as a proxy for autotrophic biomass) varied in the ranges characteristic for

16

the oligotrophic coastal waters off Rovinj (Ivančić et al., 2018). The dynamics of particulate matter was associated with freshwater input. The higher contribution from autochthonous sources was observed during the increases of autotrophic biomass. ~~The increases in particulate matter concentration were associated with freshwater input, while their enrichment with unsaturated fatty acids deriving from phytoplankton was observed during the increases of autotrophic biomass.~~ However, only in September 2017, this increase was supported by nutrients from the water column, while all other ~~less pronounced~~ increases were most likely connected to bottom waters where phytoplankton could have been supplied with nutrients ~~made available~~ through sediment resuspension. The considerable increase in the particulate matter of terrigenous origin from April to August 2018 suggested the enhanced land run-off in that period. ~~In accordance, increases in the particulate lipid matter of terrigenous origin have been observed, being generally elevated from April to August 2018. Therefore, during this investigation the dynamics of the particulate matter was most likely under the combined influence of terrigenous input and sediment resuspension, including detritus from the C. nodosa meadow.~~

In temperate Mediterranean coastal waters *C. nodosa* meadows show a clear unimodal annual growth cycle, reaching maximum development in summer, and minima during winter and a particularly active growth phase in spring (Terrados and Ross, 1992; Zavodnik et al., 1998; Agostini et al., 2003). In Saline Bay, the maximum biomass was measured in October 2017. This shift from summer to early autumn was most likely due to an intense grazing activities (Cebrian et al., 1996; Valentine and Duffy, 2006) suggested by a prevalence of visibly grazed leaves during July and August 2017. ~~In Saline Bay, the maximum growth was shifted towards early autumn. This shift was most likely due to the prevalence of massively grazed leaves during July and August 2017, suggesting an intense grazing activity in the meadows, which probably decreased during September and October 2017~~. A minimum growth occurred during late autumn/winter, as commonly observed. However, during the spring 2018, phenological parameters continued to decrease in spite of established favorable environmental conditions for growth, i.e., increase in water temperature, intensity and period of solar radiation. This decrease continued until the complete extinction of the above-ground tissue in August 2018. The belowground tissue followed a similar trend, but with less expressed changes. Still, their recognizable remnants were found after the loss of the above-ground tissues.

Organic matter and closely correlated total lipids in the sediment of *C. nodosa* rooted area changed significantly throughout the investigated period, in contrast to organic matter in non-vegetated sediment. Nevertheless, considerable ~~but the co-varying unsaturation degree suggests~~ similarity in the quality and degradation ~~degree~~ of lipid matter at both, the vegetated and the non-vegetated sites. ~~This covariation~~ indicates an important contribution of detritus imported from the meadow as a source of organic matter for prokaryotes in non-vegetated sediments. This ~~C~~close coupling ~~between the seagrass meadow and non-vegetated sites~~ could be expected due to ~~their~~site proximity and lower organic content of the non-vegetated sediment, which should enhance the dependence of prokaryotes on the imports of seagrass detritus from the adjacent meadows (Holmer et al., 2004). ~~Moreover, the non-vegetated sediment in Saline Bay could readily support the adsorption of imported organic material due to a higher proportion of mud (silt and clay) and considerably lower median grain size in comparison to the C. nodosa sediment.~~ Significant enrichment of *C. nodosa* sediment with unsaturated, more labile components only during abundant growth of meadow could be explained by more efficient entrapment of seston material within the meadow (Gacia and Duarte, 2001). Such easily utilizable organic matter, including dissolved monomeric carbohydrates, leaching out during decomposition of *C. nodosa* leaves stimulated prokaryotic growth as previously observed (Peduzzi and Herndl, 1991). ~~C. nodosa sediment was significantly enriched with organic matter, characterized by a higher contribution of unsaturated, more labile components, in comparison to the non-vegetated sediment layer only during abundant growth of meadow. Also, sestonic material from the water column is efficiently trapped and accumulates within the meadow (Gacia and Duarte, 2001), representing an additional source of labile components derived from macroalgae and C. nodosa leaves. Such easily utilizable organic matter, including dissolved monomeric carbohydrates, leaching out during decomposition of C. nodosa leaves stimulates prokaryotic growth (Peduzzi and Herndl, 1991). This effect could be observed, as prokaryotic abundance was higher in C. nodosa sediments (Fig. 8). In contrast, the lower unsaturation of lipid matter in the non-vegetated sediment can be explained by its higher instability. Resuspension and a wider oxic layer could have further suppressed the preservation of reactive and more labile organic matter in comparison to the C. nodosa sediment~~

From July 2017 to March 2018~~During the summer/early autumn 2017 and winter 2018~~, an adaptation of *C. nodosa* leaves to the decreasing light and temperature occurred~~, respectively~~.

547 ~~In both periods, an increase in unsaturation degree (primarily due to ALA increase) in order to~~

548 ~~increase the membrane fluidity was observed. From July to~~Until October 2017, the

549 temperature of the water column was still optimal for elongation of the leaves and biomass

550 increase, while the ambient light intensities were continuously decreasing. An additional

551 reduction of available light might occur from the self-shading effect due to high canopy

552 biomass, and/or shading due to epiphytic macroalgae growth. Desaturation of low and fairly

553 invariable lipids during the most active growth phase suggested an increase in the membrane

554 fluidity to optimize photosynthetic activity under low light conditions. Such physiological

555 adaptation ~~as a response to low light availability~~ was found in seagrasses living along a depth

556 gradient (Beca-Carretero et al., 2019) and macroalgae in contrasting seasons (Schmid et al.,

557 2014). ~~In contrast, i~~In late autumn 2017 ~~and sprin~~g 2018, the decrease in desaturation

558 indicated a reduced fluidity and activity of photosynthetically active membranes ~~the decrease~~

559 ~~in PUFA and UND indicated a reduced fluidity and activity of photosynthetically active~~

560 ~~membranes. The lower fluidity reduces proton leakage through the thylakoid membranes and~~

561 ~~energy consumption for their maintenance~~ (Quigg et al., 2006; Wacker et al., 2016). ~~The~~

562 ~~reduced photosynthetic activity~~This was associated with a decreased abundance of shoots and

563 above-ground biomass. ~~During the period of reduced growth and~~By shedding leaves and

564 shoots the plant further balances metabolic requirements and mobilize energy from the

565 carbohydrate reserves stored in the belowground tissue (Alcoverro et al., 2001; Lee et al.,

566 2007). During the winter, due to a sharp and continuous decrease in water temperature, rapid

567 desaturation of increasing lipids provided a cold resistance, as regularly observed in algae and

568 plants ~~data indicate a progressive trend toward highest total lipids as well as the proportions of~~

569 ~~PUFA. Rapid desaturation of increasing lipids could be attributed primarily to a sharp and~~

570 ~~continuous decrease in water temperature. An increase in the level of PUFA is considered to~~

571 ~~provide a mechanism for the thermo-adaptive regulation of membrane fluidity and cold~~

572 ~~resistance in algae and plants~~ (Terrados and Lopezjimenez, 1996; Iveša et al., 2004;

573 Upchurch, 2008).

574   In a healthy seagrass meadow, the oxygen generated by seagrass photosynthesis is

575 transported to belowground tissues to maintain an oxic microsphere around roots and

576 rhizomes, re-oxidize sulfide to non-toxic S^0, thus preventing an invasion of H_2S into the plant

577 (Pedersen et al., 1998; Holmer et al, 2005). S^0 was found in the *C. nodosa* below-ground

578 tissue during the entire investigation period, as already observed in seagrasses living in

19

sulfidic sediments (Holmer and Hasler-Sheetal, 2014; Hasler-Sheetal and Holmer, 2015). The relatively low accumulation of H_2S (< 30 μM) during the summer and early autumn 2017 indicated that H_2S was apparently rapidly recycled within the rooted area via re-oxidation by O_2 to S^0 and/or removal by precipitation with iron compounds. Most of S^0 was found in oxic layers or suboxic/anoxic boundaries, being in ranges typical for sulfidic coastal sediments (Troelsen and Jørgensen, 1982; Panutrakul et al., 2001; Pjevac et al., 2014).but also anoxic layers in July and October 2017. The oxidation of H_2S could occur spontaneously by chemical reaction with free oxygen or mediated by sulfide-oxidizing bacteria surrounding or being attached to seagrass roots (Jørgensen, 1977; Cucio et al., 2016; Ugarelli et al., 2017; Fahimipour et al., 2017). (Jørgensen, 1977). Usually S0 is the most abundant sulfide oxidation intermediate, and it accumulates to higher concentrations than other more reactive compounds (e.g. polysulfide, thiosulfate, tetrathionate, sulfite; Zopfi et al., 2004). In Saline Bay sediment S0 occurs in ranges typical for sulfidic coastal sediments (Troelsen and Jørgensen, 1982; Panutrakul et al., 2001; Pjevac et al., 2014). During the active growth of C. nodosa, the rhizosphere surrounding sediment was well supplied with photosynthetically produced oxygen due to radial oxygen leakage. Therefore, in addition to free oxygen available in pore waters, both, biotic and abiotic re-oxidation of sulfide was most likely supported by the oxygen supplied via the release from the root to the surrounding sediment (Holmer et al., 2006). Generally, thermodynamic and kinetic considerations suggest that biological oxidation far exceeds chemical oxidation of sulfide in most environments (Wasmund et al., 2017). Moreover, abundant sulfide oxidizing prokaryotes have been detected in marine sediments surrounding or attaching to seagrass roots (Cucio et al., 2016; Fahimipour et al., 2017). In November, due to the degradation of organic matter and reduced oxygen production and leakage in the rooted zone caused by *C. nodosa* senescence, the re-oxidation capacity of the sediment was greatly decreased. This resulted in considerable accumulation of H_2S (> 100 μM) which extended up to the sediment surface. During winter and early spring, H_2S production generally decreased, likely due to the reduced activity of sulfate reducing prokaryotes at lower temperatures, and the sediment gradually shifted towards a more oxidized state. H_2S detected even in within the oxic sediment and in the rooted area in February 2018 could be attributed to the sediment heterogeneity and the presence of reducing micro-niches where anaerobic metabolism could occur regardless of surrounding redox conditions (Jørgensen, 1977; Frederiksen and Glud, 2006). Moreover, it has been found that at

20

611 ~~temperatures below 15°C, organic sulfur is more important than sulfate as a sulfide source.~~
612 ~~This was explained by a higher temperature coefficient required for sulfate reduction than for~~
613 ~~other heterotrophic processes (Jørgensen, 1977).~~
614 ~~However, major differences are observed between the two periods indicated by the~~
615 ~~LA/ALA ratios. During November and December, LA and ALA proportionally decreased by~~
616 ~~keeping their ratio < 1, while during April and May ALA decreased while LA remained~~
617 ~~stable. The resulting LA/ALA > 1 suggests a decrease in the conversion of LA to ALA, which~~
618 ~~occurs in conditions of light reduction (Harris and James, 1965). This finding apparently~~
619 ~~contradicts the adaptation to low light conditions observed during C. nodosa healthy and~~
620 ~~regular growth and suggests the reduction of light below the minimum requirements for C.~~
621 ~~nodosa survival. Such conditions of light deprivation existed i~~

622 _In April 2018, C. nodosa ~~when the plant~~ had been most probably exposed to increased

623 siltation, due to a_n ~~rise~~ _increase_ in terrigenous input combined with resuspension of sediment

624 provoking elevated autotrophic growth. The intensive siltation is associated with the increased

625 light attenuation, both through the direct shading effect of suspended sediments and through

626 the promotion of phytoplankton and epiphyte growth by the associated increase in nutrients

627 (Terrados et al., 1998; Halun et al., 2002; Brodersen et al., 2015). Therefore, the increase in

628 seawater turbidity and considerable sediment re-deposition on the leaves might have severely

629 impaired the light availability and slowed down the plant's photosynthetic activity _as_

630 _indicates LA/ALA > 1 in the above-ground tissue resulting from decreased conversion of LA_

631 _to ALA (Harris and James, 1965)._ When the minimum light requirements (~14% of incidence

632 light) are not met, _C. nodosa_ intensely sheds leaves and shoots~~, while at light level of < 1% of~~

633 ~~surface solar radiation the plant dies off~~ (Collier et al., 2012). ~~This reduced~~_Such_ light

634 condition apparently persisted until May 2018 and most likely prevented the re-establishment

635 of photosynthesis and _C. nodosa_ continued to shed shoots and leaves. _The reduced_

636 _photosynthesis and therefore O_2 transport from the leaves to the rhizome-root system_

637 _probably minimized root respiration._ ~~As photosynthesis and therefore oxygen production were~~

638 ~~already reduced in April 2018, t~~_T_he maintenance of the oxic rhizosphere and the internal O_2

639 partial pressure in the lacunae further depended mainly on the diffusion of O_2 from the water

640 column. From April to June 2018, O_2 in the bottom water drastically decreased. Due to poor

641 supply, O_2 content of the belowground tissue was too low to maintain the oxic

642 microenvironment and therefore, the plant tissues became potentially accessible to sulfide

643 intrusion (Pedersen et al., 2004). ~~To reach the leaves, sulfide invasion has to exceed~~

644 ~~belowground tissue oxidation capacity and pass through these tissues, invading the meristems~~

645 ~~located at the base of the leaves, where sulfide toxicity can have drastic effects on shoot~~

646 ~~growth and survival (Greve et al., 2003; Frederiksen et al., 2008).~~

647 ~~In April 2018~~At the same time, the sediment was enriched with fresh organic matter

648 derived from increased autotrophic biomass in bottom waters. In addition to the induction of

649 the bloom, strong sediment resuspension, most likely by aeration, stimulated the intense

650 oxidation of H_2S that started to produce in the rooted zone (up to 180 μM~~, Fig. 7~~), due to

651 increased activity of sulfate reducing prokaryotes possibly triggered by the increase in

652 temperature. An increase in S^0 concentration that reached its maximum in the same layer

653 suggests a simultaneous oxidation of the produced H_2S. The sulfide oxidation probably

654 caused oxygen depletion in the rooted zone and anoxic zone extension up to the sediment

655 subsurface. In May 2018, the excess of organic matter accumulated in April 2018 was

656 degraded. The concentrations of S^0, detected only in the suboxic layer, considerably decreased

657 possibly by disproportionation or respiration by members of the sulfate reducing bacteria~~. S0~~

658 ~~disproportionating Desulfobulbaceae and S0-respiring Desulfuromonadales are frequently~~

659 ~~detected in anoxic coastal sediments~~ (Pjevac et al., 2014).

660 During June and July 2018, a sudden and significant deterioration of *C. nodosa*

661 physiological condition was indicated by the further increase in LA/ALA ratio in the leaves

662 and overall saturation of decreasing lipids in above- and below-ground tissues.~~the increase in~~

663 ~~LA/ALA ratio in the leaves and overall saturation of decreasing lipids in above- and below-~~

664 ~~ground tissues indicated a sudden and significant deterioration of the physiological conditions~~

665 ~~of C. nodosa~~. Additionally, the loss of leaf tissue negatively impacted the photosynthetic

666 carbon fixation and therefore oxygen production, including the transport of oxygen to below-

667 ground tissue (Lee and Dunton, 1997; Lee et al., 2007). The below-ground tissue that was not

668 supported by photosynthetically derived oxygen became anoxic. ~~The~~ Thus induced

669 anaerobiosis most likely caused a complete inhibition of the fatty acid desaturation chain

670 (Harris and James, 1965) and a permanent breakdown of photosynthesis leading to the final

671 decay of the above-ground biomass ~~in August 2018. As a result, the reduced renewal and~~

672 ~~storage of energy reserves in the belowground tissue led to a~~and considerable ~~depletion of~~

673 ~~reserves and~~ loss of below-ground biomass. ~~In July 2018,~~As the bottom waters were

674 completely depleted in O_2 ~~and~~ the whole plant was probably exposed to ~~H2S~~sulfides. H_2S

inhibit cytochrome c oxidase by binding to regulatory sites on the enzyme, reducing the rate of cellular respiration and leading to the chemical asphyxiation (Nichols et al., 2013).

From June to August 2018, the decomposition of organic matter, encompassing the entire sediment core, was intensified and accompanied by a large increase in H_2S concentrations (up to 1200 μM). The degradation process involved rhizomes and roots, as suggested by the apparent loss of belowground biomass. Such loss typically occurs in the first stage of plant decay, the leaching phase (Trevathan-Tackett et al., 2017). Readily available, soluble carbohydrates that largely contribute to the leachate mass (Vichkovitten and Holmer, 2004) most probably supported the increase in prokaryotic abundance observed in June and July 2018. However, the significant decrease in prokaryotic abundance that coincided with a maximum degradation of organic matter and H_2S production in August 2018 might indicate that remaining compounds were not degradable by the sulfate reduction pathway (Arndt et al., 2013) and needed the presence of prokaryotes specialized in the anaerobic degradation of refractory compounds, including cellulose and lignin.

During September and October 2018, H_2S concentrations drastically decreased, and the sediment was gradually enriched in fresh organic matter. Due to the combined effect of freshened oxygenated water inflow and resuspension which gradually deepened the oxic layer, re-oxidation of H_2S increased. Biogeochemical studies suggest that most sulfides (80 – 90 %) are eventually re-oxidized; 10 – 20 % are ultimately buried as complexes with iron (i.e. FeS, FeS_2) or with organic matter after sulfurization (Jørgensen, 1977; 1982). H_2S scavenging with iron and formation of iron sulfides might be more important in Saline Bay, since terrestrial waters are washing out *terra rossa*, rich in Fe-oxides and oxyhydroxides (Durn, 2003). For this reason, sediment cores were most likely always black with sulfuric odor, irrespective of H_2S concentrations or presence of vegetation.

Due to rapid oxygen depletion for respiratory needs and low storage capacity of lacunae, oxic conditions in belowground tissues are partially maintained by oxygen diffusing from the water column into belowground tissue (Pedersen et al., 1998; Greve et al., 2003; Sand-Jensen et al., 2005). An oxic microsphere around the seagrass roots stimulate the growth of endosymbiotic sulfide-oxidizing prokaryotes (Jensen et al., 2007), which are regular members of the seagrass microbiome (Ugarelli et al., 2017; Fahimipour et al., 2017). However, from July 2017 until March 2018, it seems that the plant was sufficiently supplied with oxygen produced either by photosynthesis and/or supplied by diffusion from the well-oxygenated

23

water column. This probably ensured the complete re-oxidation of the potentially intruding sulfide preventing root anoxia. In August 2018, the inflow of freshwaters re-oxygenated the bottom waters enabling H2S oxidation in leaves, which were, however, already in an advanced stage of decomposition. During September and October 2018, the penetration of O2 from the water column gradually led to the recovery of belowground tissue.
In addition to plant activity, sulfide intrusion into seagrasses is controlled by sediment biogeochemistry and environmental conditions (Frederiksen et al., 2006), while sulfide concentration in sediments is determined by the rate of sulfate reduction, which in turn depends on the amount of organic matter and temperature (Moeslund et al., 1994)..

5 Conclusions

Our results provide insights into the interaction of multiple stressors that have led to the meadow decay, triggered in the sensitive recruitment phase of meadow growth. Even after the improvement of the sediment conditions by the end of the summer 2018, *C. nodosa* was not able to recolonize its previously occupied areas. This finding combined with a visible alteration of the water column and sediment indicates a considerable loss of the *C. nodosa* habitat. Further research is needed to examine the fate of Saline Bay meadows and an eventual recolonization of the area.

Beyond seagrass itself, this loss had extensive consequences as it has endangered many species that depend on seagrass for food, shelter and nursery. Given the lack of data on the ecological and conservation status of the still numerous seagrass meadows along the northern Adriatic coast, the identification and monitoring of the main pressures acting on them are needed to protect such valuable habitats from degradation and extinction.

During the regular growth, from July 2017 to March 2018, C. nodosa successfully adapted to the changes of environmental conditions and prevented H2S accumulation by its re-oxidation, supplying the sediment with O2 from the water column and/or leaf photosynthesis. Our results suggest that the C. nodosa die-off was most likely triggered in April 2018 by a reduction of light availability, which severely reduced leaf photosynthesis and the oxidation capability of belowground tissue. Simultaneously, in the sediment, depletion of oxygen due to intense oxidation of H2S occurred, thus creating anoxic conditions in most of the rooted areas. This synergistic negative effect on the plant performance exposed C. nodosa to H2S intrusion. During the degradation of dying above- and belowground tissues, which culminated

in August 2018, high concentrations of H2S were produced and accumulated all over the sediment cores, including bottom waters. An improvement in the oxygen supply in September 2018 led to the re-establishment of H2S oxidation and recovery of the belowground tissue. Even if the sediment conditions improved by the end of the summer 2018, C. nodosa has not been able to recolonize its previously occupied areas in the rest of 2018 and during 2019. This finding combined with a visible alteration of the water column and sediment is suggesting a considerable habitat loss. Further research is needed to examine the fate of Saline Bay meadows remains and an eventual recolonization of the area.

References

756 Agostini, S., Pergent, G., and Marchand, B.: Growth and primary production of *Cymodocea*
757   *nodosa* in a coastal lagoon. Aquat. Bot., 76, 185-193, 2003.

759 Alcoverro, T., Manzanera, M., and Romero J.: Annual metabolic carbon balance of the
760   seagrass *Posidonia oceanica*: the importance of carbohydrate reserves. Mar. Ecol. Prog.
761   Ser., 211, 105-116, 2001.

762 Arndt, S., Jørgensen, B.B., LaRowe, D.E., Middelburg, J.J., Pancost, R.D., and Regnier, P.:
763   Quantifying the degradation of organic matter in marine sediments: A review and
764   synthesis. Earth-Science Rev., 123, 53-86, 2013.

765 Beca-Carretero, P., Guihéneuf, F., Marín-Guirao, L., Bernardeau-Esteller, J., García-Muñoz,
766   R., Stengel, D.B., and Ruiz, J.M. Effects of an experimental heat wave on fatty acid
767   composition in two Mediterranean seagrass species. Mar. Pollut. Bull., 134, 27-37, 2018.

768 Beca-Carretero, P., Guihéneuf, F., Winters, G., and Stengel, D.B.: Depth-induced adjustment
769   of fatty acid and pigment composition suggests high biochemical plasticity in the tropical
770   seagrass *Halophila stipulacea*. Mar. Ecol. Prog. Ser., 608, 105-117, 2019.

771 Borum, J., Pedersen, O., Greve, T.M. Frankovich, T.A., Zieman, J.C., Fourqurean, J.W., and
772   Madden, C.J.: The potential role of plant oxygen and sulphide dynamics in die-off events
773   of the tropical seagrass, *Thalassia testudinum*. J. Ecol., 93, 148-158, 2005.

774 Bourbonniere, R.A., and Meyers, P.A.: Sedimentary geolipid records of historical changes in
775   the watersheds and productivities of Lakes Ontario and Erie. Limnol. Oceanogr., 41, 352-
776   359, 1996.

777 Brodersen, K.E., Lichtenberg, M., Paz, L-C., and Kühl, M.: Epiphyte-cover on seagrass
778   (*Zostera marina* L.) leaves impedes plant performance and radial O_2 loss from the bellow-
779   ground tissue. Front. Mar. Sci., 2, 58 doi: 10.3389/fmars.201500058, 2015.

780 Cancemi, G., Buia, M.C., and Mazzella, L.: Structure and growth dynamics of *Cymodocea*
781   *nodosa* meadows. Sci. Mar., 66: 365-373, 2002.

782 Canfield, D.E., Jørgensen, B.B., Fossing, H., Glud, R., Gundersen, J., Ramsing, N.B.,
783   Thamdrup, B., Hansen, J.W., Nielsen, L.P., and Hall, P.O.J.: Pathways of organic carbon
784   oxidation in three continental margin sediments. Mar. Geol., 113, 27-40, 1993.

785 Capone, D.G., and Kiene, R.P.: Comparison of microbial dynamics in marine and freshwater
786   sediments: Contrasts in anaerobic carbon catabolism. Limnol. Oceanogr., 33, 725-749,
787   1988.

788 Carlson, P.R., Yarbro, L.A., and Barber, T.R.: Relationship of sediment sulfide to mortality of
789   *Thalassia testudinum*, Florida Bay. Bull. Mar. Sci., 54, 733-746, 1994.

790 Cebrian, J., Duarte, C.M., and Marbà, N.: Herbivory on the seagrass *Cymodocea nodosa*
791   (Ucria) Ascherson in contrasting Spanish Mediterranean habitats. J. Exp. Mar. Biol. Ecol.,
792   204, 103-111, 1996.

793 Cline, J.D.: Spectrophotometric determination of hydrogen sulfide in natural waters. Limnol.
794   Oceanogr., 14, 454-458, 1969.

795 Collier, C.J., Lavery, P.S., Masini, R.J., and Ralph, P.J.: Shade-induced response and recovery
796   of the seagrass *Posidonia sinuosa*. J. Exp. Mar. Biol. Ecol., 370, 89-103, 2009.

797 Collier, J.C., Waycott, M., and Giraldo Ospina, A.: Responses of four Indo-West Pacific
798   seagrass species to shading. Mar. Pollut. Bull., 65, 342-354, 2012.

799 Costa, M.M., Barrote, I., Silva, J., Olivé, I., Alexandre, A., Albano, S., and Santos, R.:
800   Epiphytes modulate *Posidonia oceanica* photosynthetic production, energetic balance,
801   antioxidant mechanisms, and oxidative damage. Front. Mar. Sci. 2:111, 2015.

802 Cranwell, P.A., Eglinton, G., and Robinson, N.: Lipids of aquatic organisms as potential
803   contributors to lacustrine sediments. Org. Geochem., 11, 513-527, 1987.

804 Cúcio, C., Engelen, A.H., Costa, R., and Muyzer, G.: Rhizosphere Microbiomes of European
805   Seagrasses Are Selected by the Plant, But Are Not Species Specific. Front. Microbiol., 7,
806   440. doi: 10.3389/fmicb.2016.00440, 2012.

807 Duarte, C.M., Kennedy, H., Marbà, N., Gacia, E., Fourqurean, J.W., Beggins, J., Barrón, C.,
808   Apostolaki, E.T.: Seagrass community metabolism: Assessing the capacity of seagrass
809   meadows for carbon burial: Current limitations and future strategies. Ocean Coast. Manag.,
810   83, 32-38, 2013.

811 Durn, G.: *Terra Rossa* in the Mediterranean Region: Parent Materials, Composition and
812   Origin. Geologia Croatica, 56, 83-100, 2003.

813 Epstein, S.S., and Rossel J.: Enumeration of sandy sediment bacteria: search for optimal
814   protocol. Mar. Ecol. Prog. Ser., 117, 289-298, 1995.

815 Fahimipour, A.K., Kardish, M.R., Lang, J.M., Green, J.L., Eisen, J.A., and Stachowicz, J.J.:
816   Global-Scale Structure of the Eelgrass Microbiome. Appl. Environ. Microbiol., 83,
817   e03391-16, 2017.

818 Folk, R.L.: The distinction between grain size and mineral composition in sedimentary-rock
819   nomenclature. J. Geol., 62, 344-359, 1954.

820 Frederiksen, M.S., Holmer, M., Pérez, M., Invers, O., Ruiz, J.M., and Knudsen, B.: Effect of
821   increased sediment sulfide concentrations on the composition of stable sulfur isotopes
822   (δ^{34}S) and sulfur accumulation in the seagrasses *Zostera marina* and *Posidonia oceanica*.
823   J. Exp. Mar. Biol. Ecol., 358, 98-109, 2008.

824 Frederiksen, M.S., and Glud, R.N.: Oxygen dynamics in the rhizosphere of *Zostera marina*: A
825   two-dimensional planar optode study. Limnol. Oceanogr., 51, 1072-1083, 2006.

826 Gacia, E., and Duarte, C.M.: Sediment Retention by a Mediterranean *Posidonia oceanica*
827   Meadow: The Balance between Deposition and Resuspension. Estuar. Coast. Shelf. Sci.,
828   52, 505–514, 2001.

829 Gangi, A.F.: Permeability of unconsolidated sands and porous rocks. J. Geophys. Res. –Solid,
830   90, 3099-3104, 1985.

831 Gao, G., Clare, A.S., Chatzidimitriou, E., Rose, C., and Caldwell, G.: Effects of ocean
832   warming and acidification, combined with nutrient enrichment, on chemical composition
833   and functional properties of *Ulva rigida*. Food Chem., 258, 71-78, 2018.

834 Greve, T.M., Borum, J., and Pedersen, O.: Meristematic oxygen variability in eelgrass
835   (*Zostera marina*). Limnol. Oceanogr., 48, 210-216, 2003.

836 Halun, Z., Terrados, J., Borum, J., Kamp-Nielsen, J., Duarte, C.M., and Fortes, M.D.:
837   Experimental evaluation of the effects of siltation-derived changes in sediment conditions
838   on the Philippine seagrass *Cymodocea rotundata*. J. Exp. Mar. Biol. Ecol., 279, 73-87,
839   2002.

840 Harris, R.V., and James, A.T.: Linoleic and α-linolenic acid biosynthesis in plant leaves and a
841   green alga. Biochim. Biophys. Acta, 106, 456-464, 1965.

842 Hasler-Sheetal, H., and Holmer, M.: Sulfide intrusion and detoxification in the seagrass
843   *Zostera marina*. Plos One 10(6): e0129136, 2015.

844 Hendriks, I.E., Sintes, T., Bouma, T.J., and Duarte, C.M.: Experimental assessment and
845   modeling evaluation of the effects of the seagrass *Posidonia oceanica* on flow and particle
846   trapping. Mar. Ecol. Prog. Ser., 356, 163-173, 2008.

847 Holm-Hansen, O., Lorenzen, C. J., Holmes, R. W., and Strickland, J. D. H.: Fluorometric
848   determination of chlorophyll. J. Conseil., 301, 3-15, 1965.

849 Holmer, M., Duarte, C.M., Boschker, H.T.S., and Barrón, C.: Carbon cycling and bacterial
850   carbon sources in pristine and impacted Mediterranean seagrass sediments. Aquat. Microb.
851   Ecol., 36, 227-237, 2004.

852 Holmer, M., and Hasler-Sheetal, H.: Sulfide intrusion in seagrasses assessed by stable

853   isotopes- a synthesis of current results. Front. Mar. Sci., doi: 10.3389/fmars.2014.00064,

854   2014.

855 Holmer, M., and Nielsen, S.L.: Sediment sulfur dynamics related to biomass-density pattern

856   in *Zostera marina* (eelgrass) beds. Mar. Ecol. Prog. Ser., 146, 163-171, 1997.

857 Holmer, M., Frederiksen, M.S., and Møllegaard, H.: Sulfur accumulation in eelgrass (*Zostera*

858   *marina*) and effect of sulfur on eelgrass growth. Aquat. Bot., 81, 367-379, 2005.

859 Holmer, M., Pedersen, O., and Ikejima, K.: Sulfur cycling and sulfide intrusion in mixed

860   Southeast Asian tropical seagrass meadows. Bot. Mar., 49, 91-102, 2006.

861 Ivančić, I., Paliaga, P., Pfannkuchen, M., Đakovac, T., Najdek, M., Steiner, P., Korlević, M.,

862   Markovski, M., Baričević, A., Smodlaka Tanković, M., and Herndl, G.J.: Seasonal

863   variations in extracellular enzymatic activity in marine snow-associated microbial

864   communities and their impact on the surrounding water. FEMS Microbiol. Ecol., 94,

865   fyi198, 2018.

866 Iveša, Lj., Blažina, M., and Najdek, M.: Seasonal variations in fatty acid composition of

867   *Caulerpa taxifolia* (M. Vahl.) C. Ag. in the northern Adriatic Sea (Malinska, Croatia). Bot.

868   Mar., 47, 209-214, 2004.

869 Jørgensen, B.B.: The sulfur cycle of a coastal marine sediment (Limfjorden, Denmark).

870   Limnol. Oceanogr., 22, 814-832, 1977.

871 Jørgensen, B.B.: Mineralization of organic matter in the sea bed - the role of sulphate

872   reduction. Nature, 296, 643-645, 1982.

873 Koch, M.S., and Erskine, J.M.: Sulfide as a Phytotoxin to the Tropical Seagrass *Thalassia*

874   *testudinum*: Interactions with Light, Salinity and Temperature. J. Exp. Mar. Biol. Ecol.,

875   266, 81-95, 2001.

876 Krause-Jensen, D., Carstensen, J., Nielsen, S.L., Dalsgaard, T., Christensen, P.B., Fossing, H.,

877   and Rasmussen, M.B.: Sea bottom characteristics affect depth limits of eelgrass *Zostera*

878   *marina*. Mar. Ecol. Prog. Ser., 425, 91-102, 2011.

879 Lee, K-S., and Dunton, K.H.: Diurnal changes in pore water sulfide concentrations in the

880   seagrass *Thalassia testudinum* beds: the effects of seagrasses on sulfide dynamics. J. Exp.

881   Mar. Biol. Ecol., 255, 201-214, 2000.

882 Lee, K-S., Park, S.R., and Kim, Y.K.: Effects of irradiance, temperature, and nutrients on

883   growth dynamics of seagrasses: A review. J. Exp. Mar. Biol. Ecol., 350, 144-175, 2007.

884　Marbà, N., and Duarte, C.M.: Growth and sediment space occupation by seagrass *Cymodocea*

885　　　*nodosa* roots. Mar. Ecol. Prog. Ser., 224, 291-298, 2001.

886　Mascaró, O., Valdemarsen, T., Holmer, M., Pérez, M., and Romero, J.: Experimental

887　　　manipulation of sediment organic content and water column aeration reduces *Zostera*

888　　　*marina* (eelgrass) growth and survival. J. Exp. Mar. Biol. Ecol., 373, 26-34, 2009.

889　Micromeritics: SediGraph 5100 particle size analysis system operator' manual. Micromeritics

890　　　Instrument Corporation, Norcross, 2002.

891　Moeslund, L., Thamdrup, B., and Jørgensen, B.B.: Sulfur and iron cycling in a coastal

892　　　sediment—radiotracer studies and seasonal dynamics. Biogeochemistry, 27, 129-152,

893　　　1994.

894　Nicholls, P., Marshall, D.C., Cooper, C.E., and Wilson, M.T.: Sulfide inhibition of and

895　　　metabolism by cytochrome c oxidase. Biochem. Soc. Transact., 41, 1312-1316, 2013.

896　Orlando-Bonaca, M., Francé, J., Mavrič, B., Grego, M., Lipej, L., Flander Putrle, V., Šiško,

897　　　M., and Falace, A.: A new index (MediSkew) for the assessment of the *Cymodocea nodosa*

898　　　(Ucria) Ascherson meadow's status. Mar. Environ. Res., 110, 132-141, 2015.

899　Orlando-Bonaca, M., Francé, J., Mavrič, B., and Lipej, L.: Impact of the Port of Koper on

900　　　Cymodocea nodosa meadow. Annales, 29, 187-194, 2019.

901　Orth, R.J., Carruthers, T.J.B., Dennison, W.C., Duarte, C.M., Fourqurean, J.W., Heck Jr.,

902　　　K.L., Hughes, A.R., Kendrick, G.A., Kenworthy, E.J., Olyarnik, S., Short, F.T., Waycott,

903　　　M., and Williams, S.L.: A Global Crisis for Seagrass Ecosystems. BioScience, 56, 987-

904　　　996, 2006.

905　Panutrakul, S., Monteny, F., and Baeyens, W.: Seasonal Variations in Sediment Sulfur

906　　　Cycling in the Ballastplaat Mudflat, Belgium. Estuaries 24, 257-265, 2001.

907　Pedersen, M.F., Duarte, C.M., and Cebrián, J.: Rates of changes in organic matter and nutrient

908　　　stocks during seagrass *Cymodocea nodosa* colonization and stand development. Mar. Ecol.

909　　　Prog. Ser., 159, 29-36, 1997.

910　Pedersen, O., Borum, J., Duarte, C.M., and Fortes, M.D.: Oxygen dynamics in the rhizosphere

911　　　of *Cymodocea rotundata*. Mar. Ecol. Prog. Ser., 169, 283-288, 1988.

912　Pedersen, O., Binzer, T., and Borum, J.: Sulphide intrusion in eelgrass (*Zostera marina* L.).

913　　　Plant Cell Environ., 27, 595-602, 2004.

Peduzzi, P., and Herndl, G.J.: Decomposition and significance of seagrass litter (*Cymodocea nodosa*) for the microbial food web in coastal waters (Gulf of Trieste, Northern Adriatic Sea). Mar. Ecol. Prog. Ser., 71, 163-174, 1991.

Pérez, M., Invers, O., Ruiz Fernandez, J.M., Frederiksen, M., and Holmer, M.: Physiological responses of the seagrass *Posidonia oceanica* to elevated organic matter content in sediments: An experimental assessment. J. Exp. Mar. Biol. Ecol., 344,149-160, 2007.

Pirini, M., Manuzzi, M.P., Pagliarani, A., Trombetti, F., Borgatti, A.R., and Ventrella, V.: Changes in fatty acid composition of *Mytilus galloprovincialis* (Lmk) fed on microalgal and wheat germ diets. Comp. Biochem. Physiol. B, 147, 616-626, 2007.

Pjevac, P., Kamyshny Jr., A., Dyksma, S., and Mussmann, M.: Microbial consumption of zero-valence sulfur in marine benthic habitats. Environ. Microbiol., 16, 3416-3430, 2014.

Porter, K.G., and Feig, Y.S.: The use of DAPI for identification and counting aquatic microflora. Limnol. Oceanogr., 25, 943-984, 1980.

Quigg, A., Kevekordes, K., Raven, J., and Beardall, J.: Limitations on microalgal growth at very low photon fluency rates: the role of energy slippage. Photosynth. Res., 88, 299-310, 2006.

Rogowska, J., Sychowska, J., Cieszynska-Semenowicz, M., and Wolska, L.: Elemental sulfur in sediments: analytical problems. Environ. Sci. Pollut. Res., 23, 24871-24879, 2016.

Samper-Villarreal, J., Lovelock, C.E., Saunders, M.I., Roelfsema, C., and Mumby, P.J.: Organic carbon in seagrass sediment is influenced by seagrass canopy complexity, turbidity, wave height, and water depth. Limnol. Oceanogr., 61, 938-952, 2016.

Sand-Jensen, K., Pedersen, O., Binzer, T., and Borum, J.: Contrasting Oxygen Dynamics in the Freshwater Isoetid *Lobelia dortmanna* and the Marine Seagrass *Zostera marina*. Ann. Bot., 96, 613-623, 2005.

Schmid, M., Guihéneuf, F., and Stengel, D.B.: Fatty acid contents and profiles of 16 macroalgae collected from the Irish Coast at two seasons. J. Appl. Phycol., 26, 451-463, 2014.

Short, F.T., Polidoro, B., Livingstone, S.R., Carpenter, K.E., Bandeira, S., Bujang, J.S., Calumpong, H.P., Carruthers, T.J.B., Coles, R.G., Dennison, W.C., Erftemeijer, P.L.A., Fortes, M.D., Freeman, A.S., Jagtap, T.G., Kamal, A.M., Kendrick, G.A., Kenworthy, W.J., La Nafie, Y.A., Nasution, I.M., Orth, R.J., Prathep, A., Sanciangco, J.C., van

Tussenbroek, B., and Vergara, S.G.: Extinction risk assessment of the world's seagrass
species. Biol. Conserv., 144, 1961-1971, 2011.

Sousa, A.I., Calado, R., Cleary, D.F.R., Nunes, C., Coimbra, M.A., Serôdio, J., and Lillebø,
A.I.: Effect of spatio-temporal shifts in salinity combined with other environmental
variables on the ecological processes provided by *Zostera noltii* meadows. Sci. Rep., 7,
1336, 2017.

Strickland, J.D.H., and Parsons, T.R.: A practical handbook of seawater analysis. Bull. Fish.
Res. Board. Can., 167,1-310, 1972.

Terrados, J., and Lopez-Jimenez, J.A.: Fatty acid composition and chilling resistance in the
green alga *Caulerpa prolifera* (Forrskal) Lamouroux (Chlorophyta, Caulerpales).Biochem.
Molecul. Biol. Internatl., 39, 863-869, 1996.

Terrados, J., Duarte, C.M., Fortes, M.D., Borum, J., Agawin, N.S.R., Bach, S., Thampanya,
U., Kamp-Nielsen, L., Kenworthy, W.J., Geertz-Hansen, O., and Vermaat, J.: Changes in
Community Structure and Biomass of Seagrass Communities along Gradients of Siltation
in SE Asia. Estuar. Coast. Shelf Sci., 46, 757-768, 1998.

Terrados, J., and Ros, J.D.: Growth and primary production of *Cymodocea nodosa* (Ucria)
Ascherson in a Mediterranean coastal lagoon: the Mar Menor (SE Spain). Aquat. Bot., 43,
63-74, 1992.

Trevathan-Tackett, S.M., Seymour, J.R., Nielsen, D.A., Macreadie, P.I., Jeffries, T.C.,
Sanderman, J., Baldock, J., Howes, J.M., Steven, A.D.L., and Ralph, P.J.: Sediment anoxia
limits microbial-driven seagrass carbon remineralization under warming conditions. FEMS
Microbiol. Ecol., 93,fix033, 2017.

Troelsen, H., and Jørgensen, B.B.: Seasonal dynamics of elemental sulfur in two coastal
sediments. Estuar. Coast. Shelf Sci., 15, 255-266, 1982.

Tuya, F., Martín, J.A., and Luque, A.: Impact of a marina construction on seagrass bed at
Lanzarote (Canary Islands). J. Coast. Conserv., 8, 157-162, 2002.

Tuya, F., Ribeiro-Leite, L., Arto-Cuesta, N., Coca, J., Haroun, R., and Espino, F.: Decadal
changes in the structure of *Cymodocea nodosa* seagrass meadows: Natural vs. human
influences. Estuar. Coast. Shelf Sci., 137, 41-49 (2014).

Ugarelli, K., Chakrabarti, S., Laas, P., and Stingl, U.: The seagrass holobiont and its
microbiome. Microorganisms 5, 81, 2017.

976 Upchurch, R.G.: Fatty acid unsaturation, mobilization, and regulation in the response of plants
977 to stress. Biotechnol. Lett., 30, 967-977, 2008.

978 Valentine, J.F., and Duffy, J.E.: The central role of grazing in seagrass ecology. In:
979 Seagrasses: Biology, Ecology and Conservation, Springer, Netherlands, pp 431-501, 2006.

980 Vaquer-Sunyer, R., and Duarte, C.M.: Thresholds of hypoxia for marine biodiversity. PNAS,
981 105, 15452-15457, 2008.

982 Vaquer-Sunyer, R., and Duarte, C.M.: Sulfide exposure accelerates hypoxia-driven mortality.
983 Limnol. Oceanogr., 55, 1075-1082, 2010.

984 Viso, A.C., Pesando, D., Bernard, P., and Marty, J.C.: Lipid components of the Mediterranean
985 seagrass *Posidonia oceanica*. Mar. Pollut. Bull., 34, 381-387, 1993.

986 Vichkovitten, T., and Holmer, M.: Contribution of plant carbohydrates to sedimentary carbon
987 mineralization. Org. Geochem., 35,1053-1066, 2004.

988 Wacker, A., Piepho, M., Harwood, J.L., Guschina, I.A., and Arts, M.T.: Light-induced
989 changes in fatty acid profiles of specific lipid classes in several freshwater phytoplankton
990 species. Front. Plant Sci., 7, 264, 2016.

991 Widdows, J., Pope, N.D., Brinsley, M.D., Asmus, H., and Asmus, R.M.: Effects of seagrass
992 beds (*Zostera noltii* and *Z. marina*) on near-bed hydrodynamics and sediment
993 resuspension. Mar. Ecol. Prog. Ser., 358, 125-136, 2008.

994 Zavodnik, N., Travizi, A., and De Rosa, S.: Seasonal variations in the rate of photosynthetic
995 activity and chemical composition of the seagrass *Cymodocea nodosa* (Ucr.) Asch. Sci.
996 Mar., 62, 301-309, 1998.
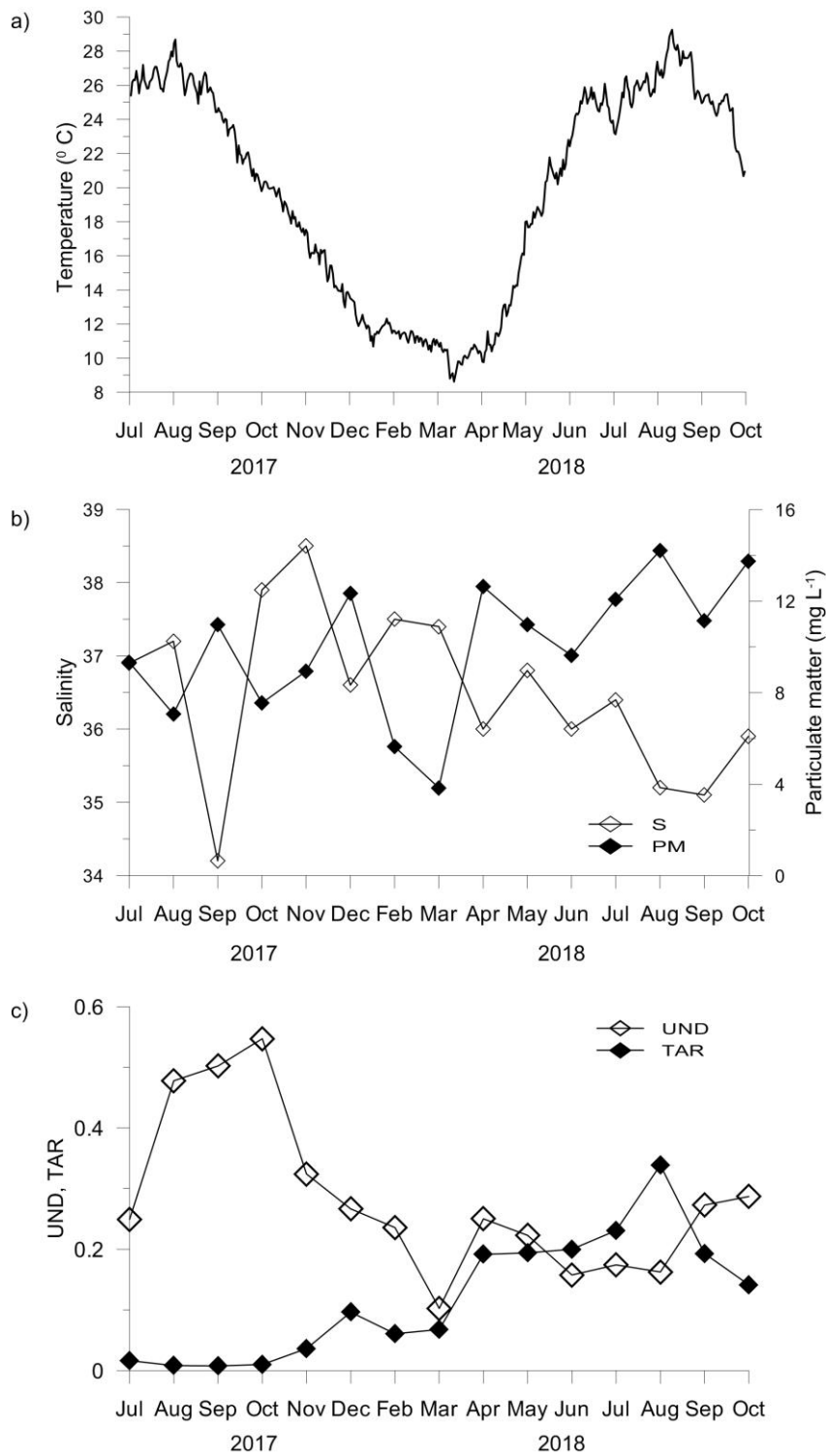
Figure 1. Temperature (a); salinity (b), particulate matter concentration (b); unsaturation degree (UND) and terrestrial to aquatic ratio (TAR) of the particulate lipid matter (c) in seawater.

35
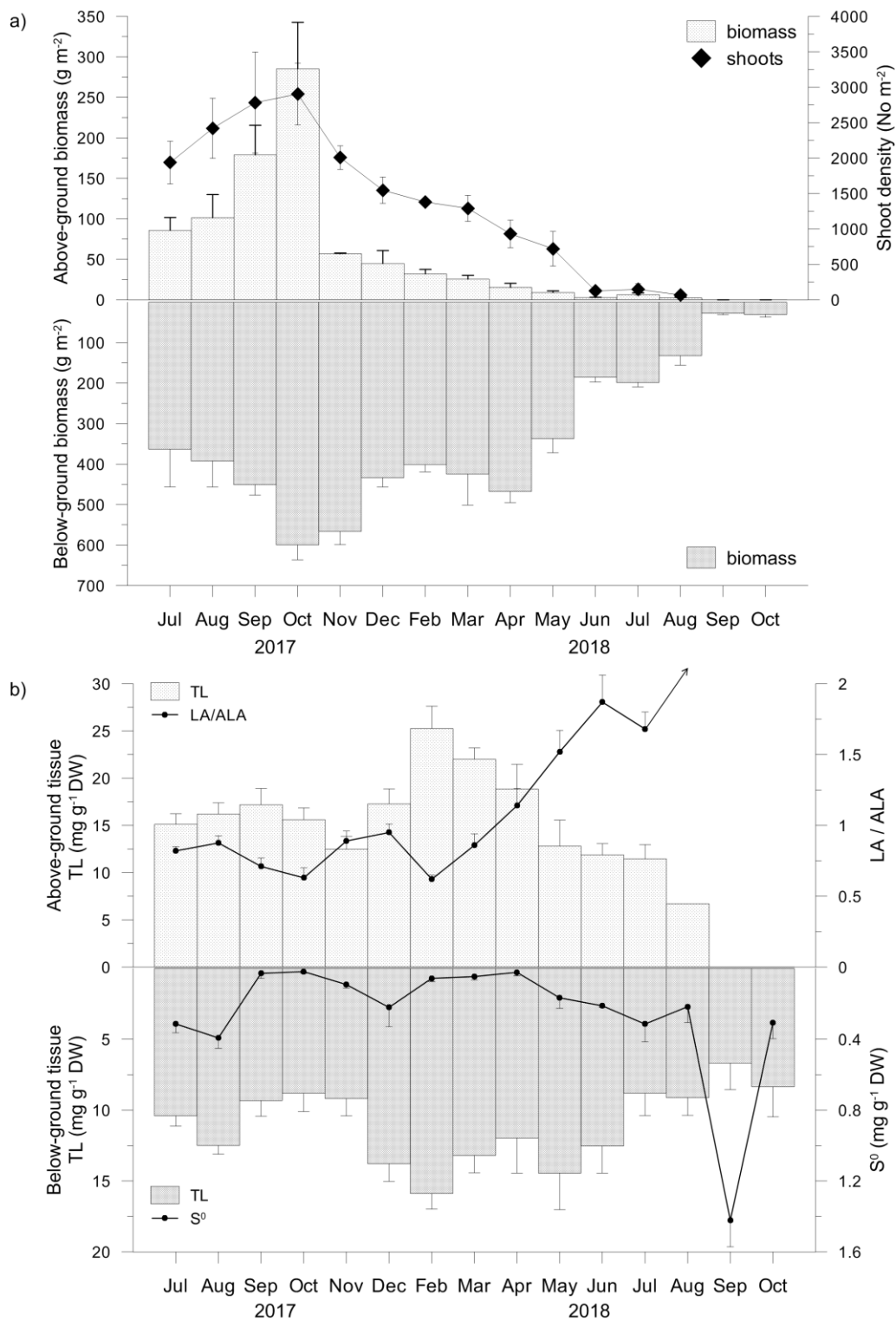
1002

Figure 2. Above- and below-ground tissue biomasses and shoot density (a), total lipid
concentrations (TL) and linoleic to α-linolenic fatty acids ratios (LA/ALA, an arrow indicates
an infinite value) in above-ground tissue and TL and approximated concentrations of
elemental sulfur (S^0) in below-ground tissue (b).
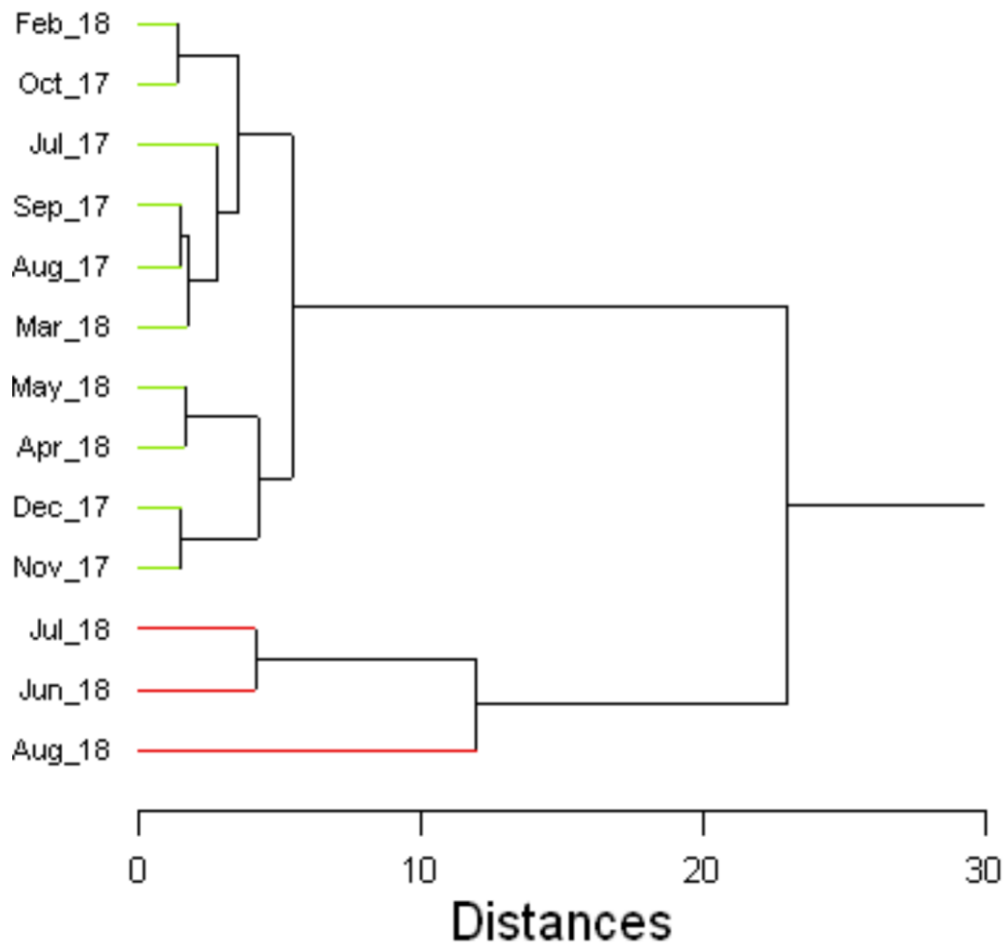
1007

1008   Figure 3. Cluster analysis dendrogram of fatty acid composition of *C. nodosa* leaves.

1009   Summary statistics is given in Table S3.
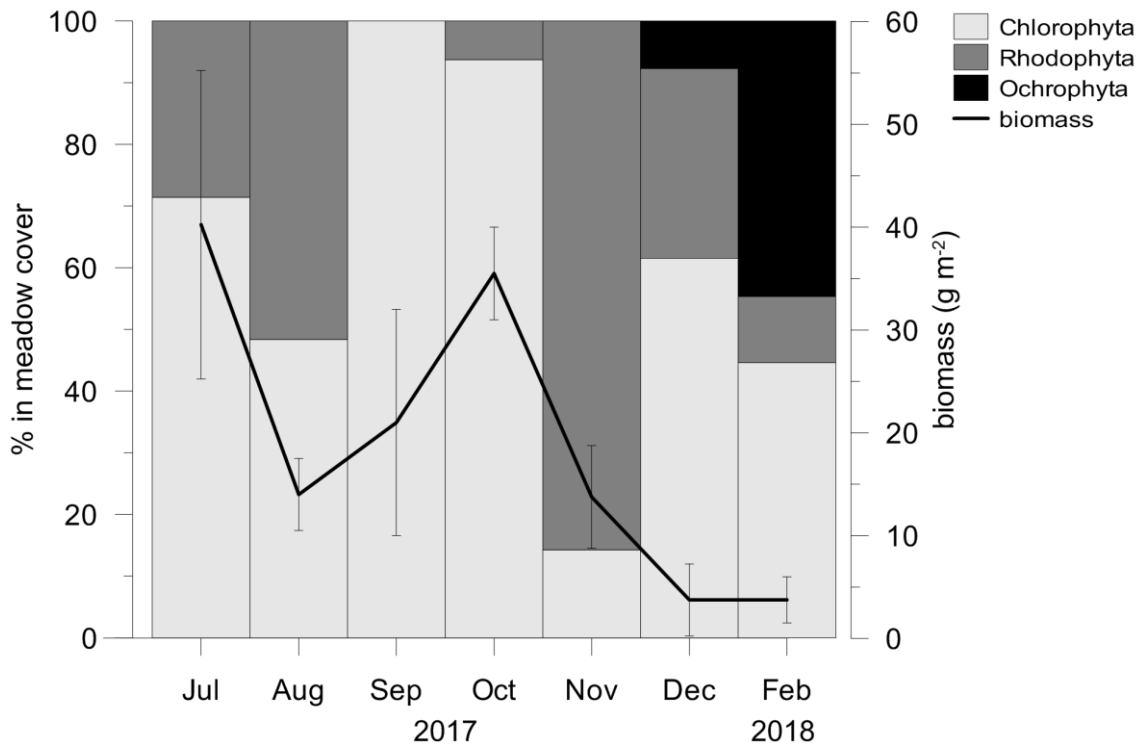
Figure 4. The contribution of macroalgal phyla in a meadow cover and total macroalgal biomass. After February 2018 macroalgae were no longer present in the *C. nodosa* meadow.
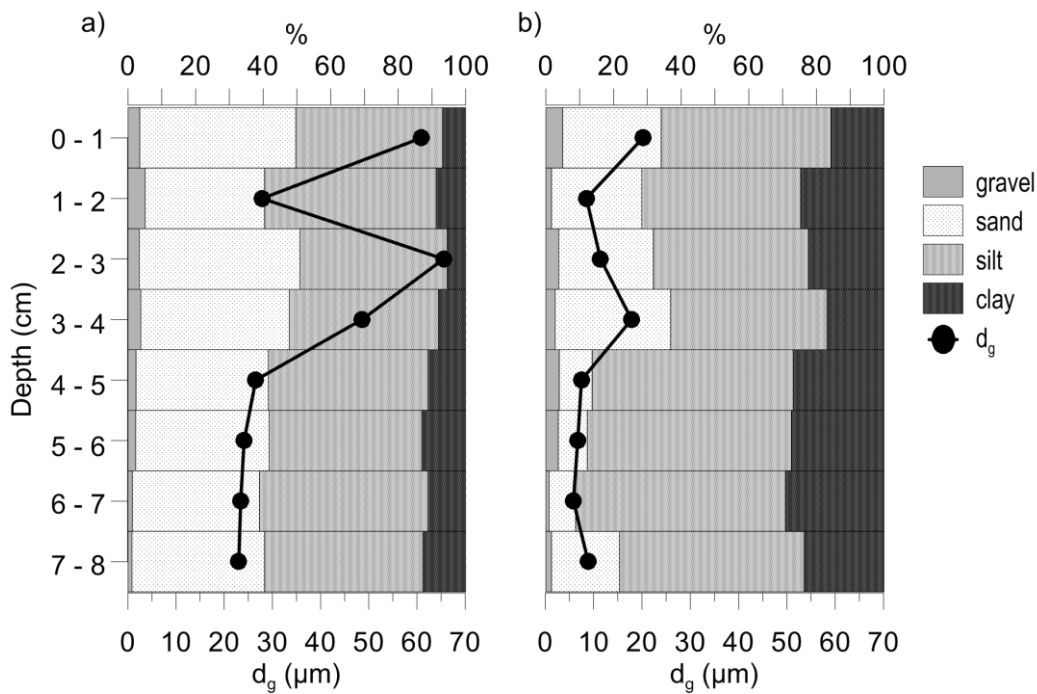
Figure 5. Granulometric composition and median grain size (d_g) of vegetated (a) and non-vegetated sediment (b).
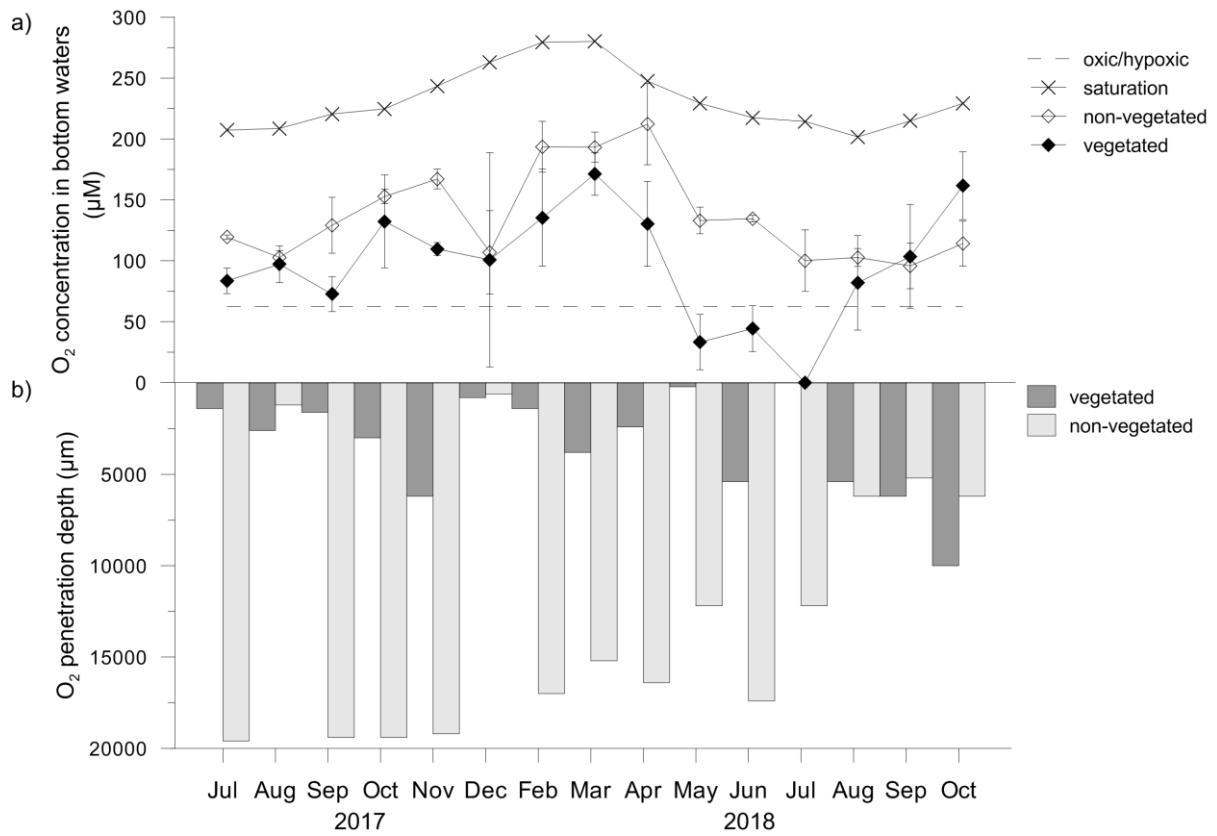
Figure 6. Oxygen concentrations (O_2) in bottom waters (a) and O_2 penetration depths (b) above and in vegetated and non-vegetated sediment, respectively. O_2 at the saturation level was calculated according to the temperature and salinity measured in seawater at the sampling dates; O_2 at the hypoxic frontier (~ 62.5 µM) was taken from Vaquer-Sanyer and Duarte (2008).
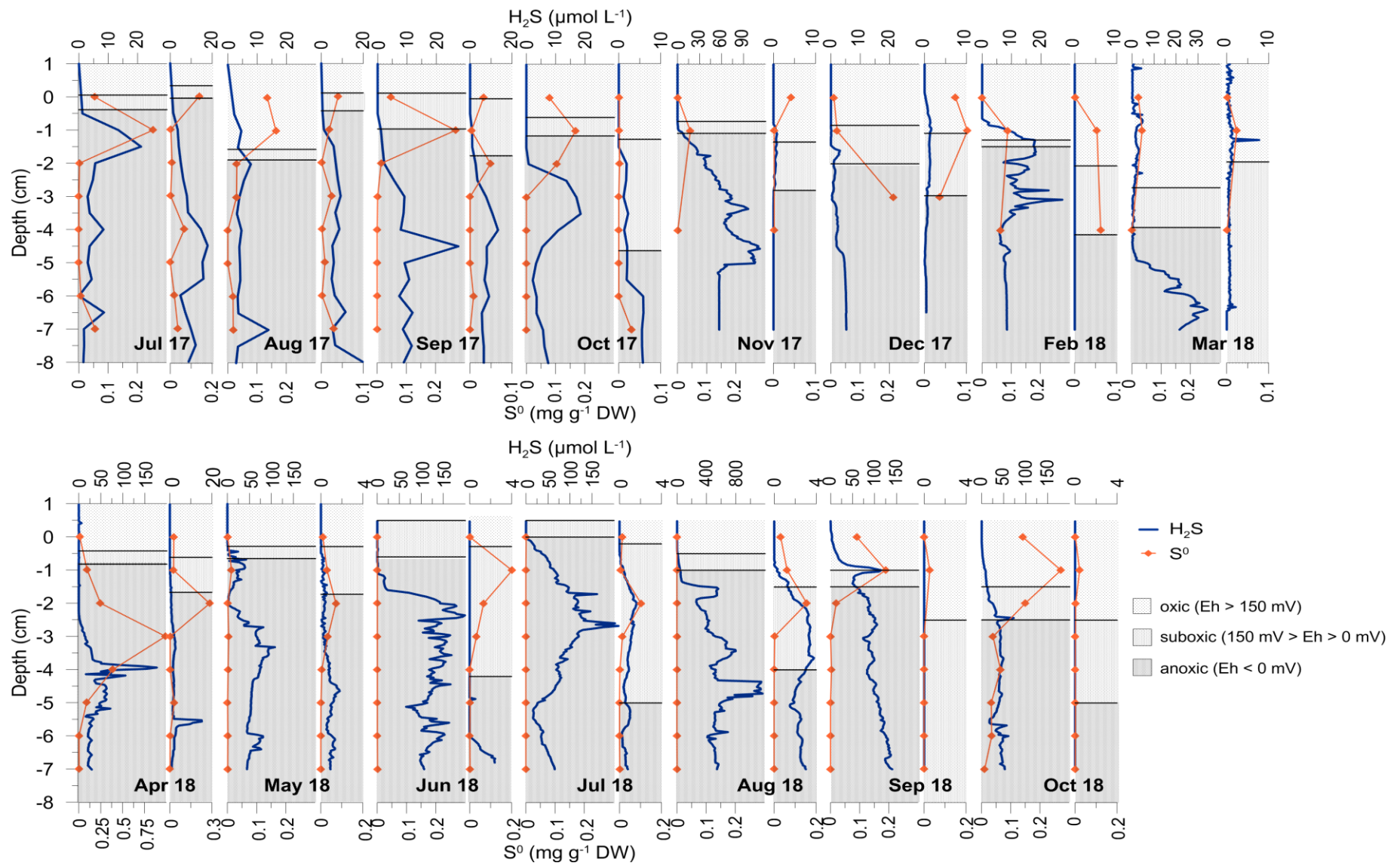
Figure 7. Depth profiles of H_2S and S^0 concentrations in vegetated and non-vegetated sediment (adjacent narrow graphs). The redox potential (Eh) in both sediments is shown as areas corresponding to oxic (Eh > 150 mV), suboxic (150 > Eh > 0 mV) and anoxic (Eh < 0 mV) conditions.
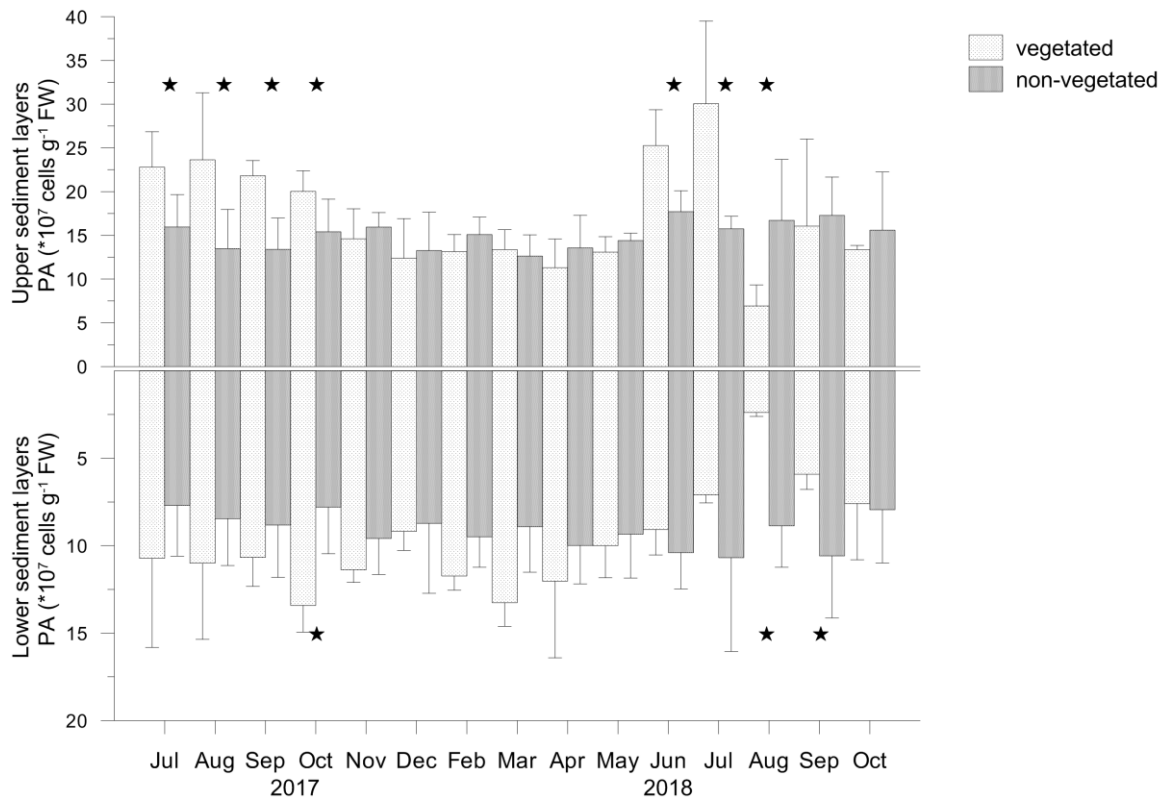
Figure 8. Prokaryotic abundance (PA) in the upper (0 - 4 cm) and lower (5 - 8 cm) layers of vegetated and non-vegetated sediments; significant differences in PA between the sediments are indicated by asterisks.
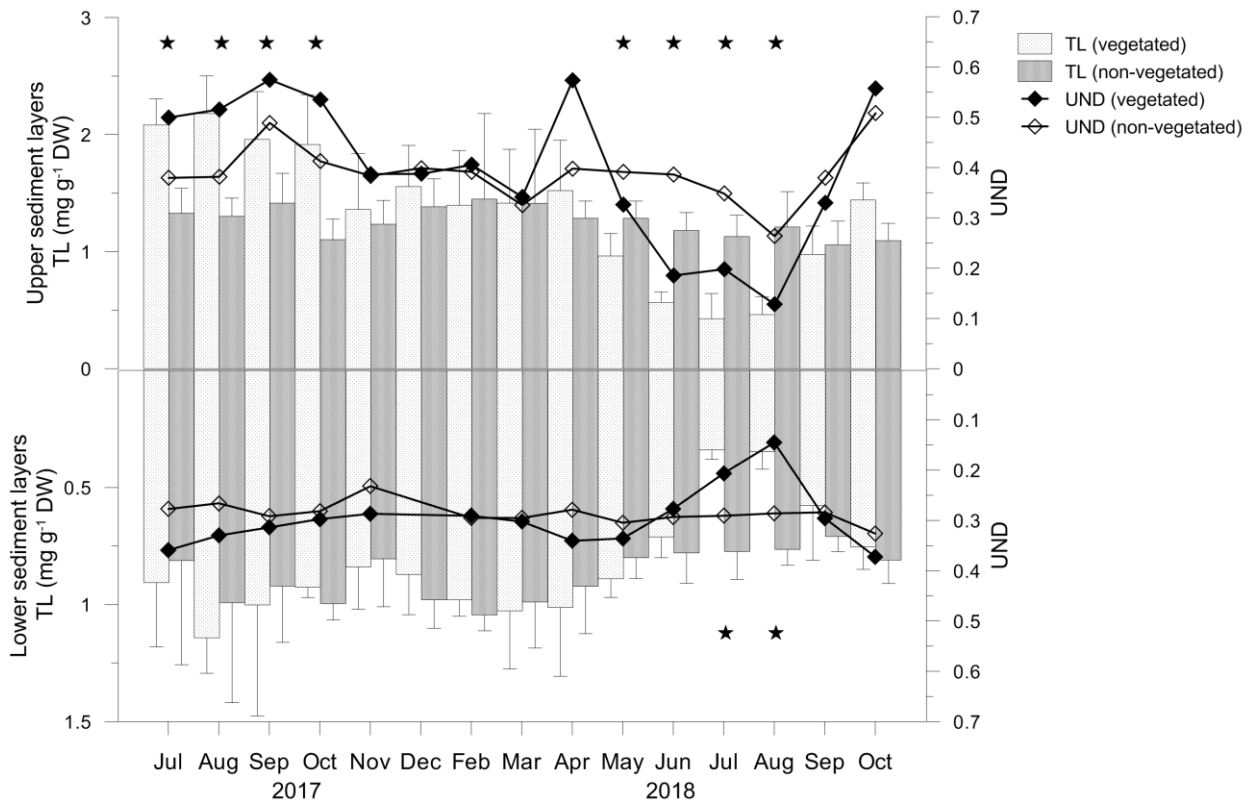
Figure 9. Total lipid concentrations (TL) and unsaturation degree (UND) in the upper (0 - 4 cm) and lower (5 - 8 cm) layers of vegetated and non-vegetated sediments. Significant differences in TL between the sediments are indicated by asterisks.
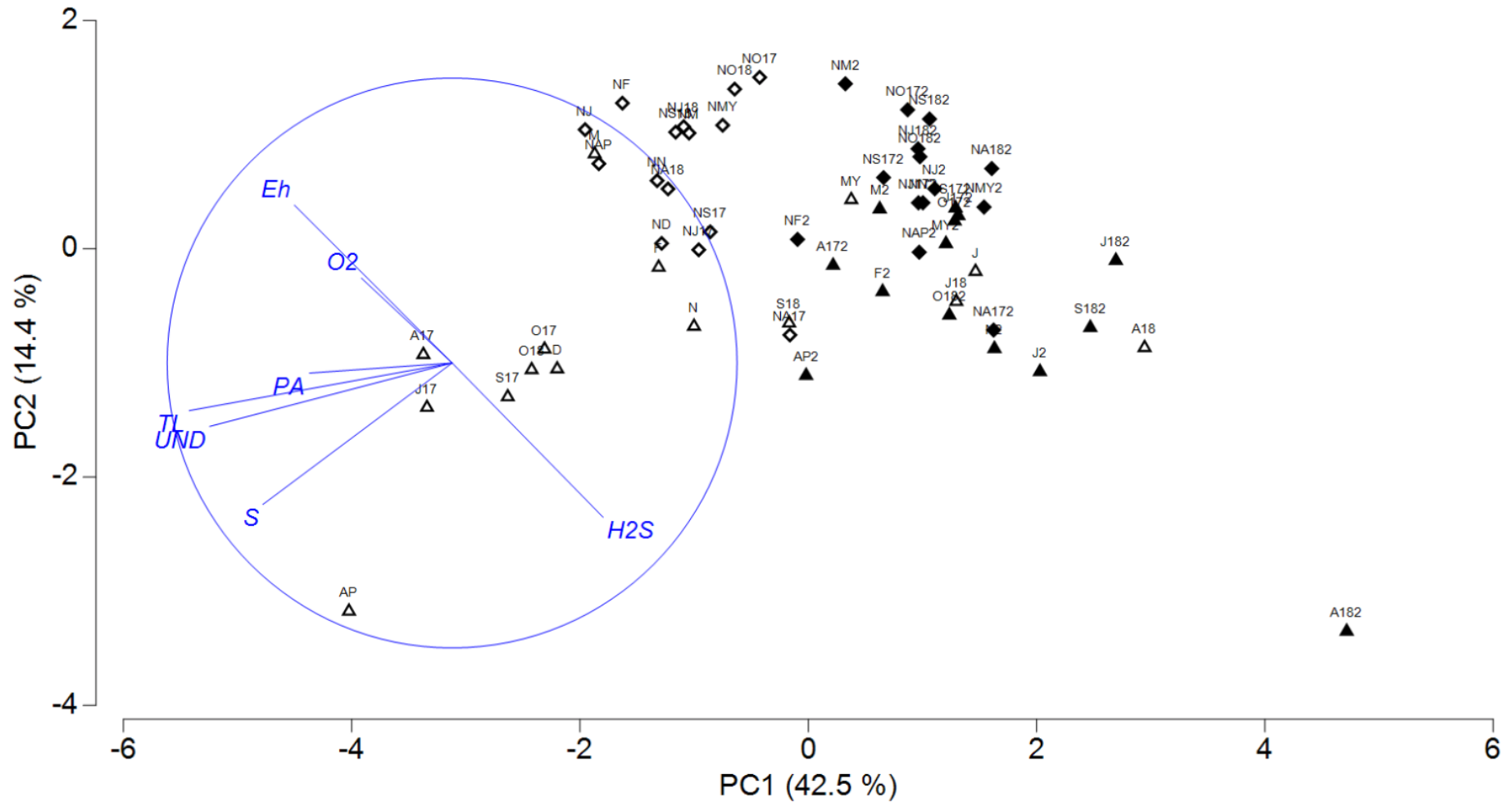
Figure 10. PCA plot of redox potential (Eh), oxygen (O_2), hydrogen sulfide (H_2S), sulfur (S), total lipids (TL) and prokaryotes (PA) concentrations and unsaturation degree (UND) in the upper ($0 - 4$ cm; $\triangle$, $\diamondsuit$) and lower ($5 - 7$ cm; $\blacktriangle$, $\blacklozenge$) layers of vegetated and non-vegetated sediments, respectively. Projections of variables are given in circles.